Zoosyst. Evol. 101 (2) 2025, 509–532 | DOI 10.3897/zse.101.144277

PENSOFT

für Naturkunde MUSEUM FÜR NATURKUNDE BERLIN

Three new species of the millipede genus *Enghoffosoma* Golovatch, 1993 from Thailand (Diplopoda, Polydesmida, Paradoxosomatidae)

Theemaporn Benchapong[1], Henrik Enghoff[2], Natdanai Likhitrakarn[3], Ratmanee Chanabun[4,5], Anuwat Aoonkum[4,5], Ruttapon Srisonchai[1,5]

1 *Department of Biology, Faculty of Science, Khon Kaen University, Khon Kaen, 40002 Thailand*
2 *Natural History Museum of Denmark, University of Copenhagen, Universitetsparken 15, DK-2100 København Ø, Denmark*
3 *Program of Agriculture, Faculty of Agricultural Production, Maejo University, Chiang Mai 50290, Thailand*
4 *Program in Animal Science, Faculty of Agricultural Technology, Sakon Nakhon Rajabhat University, Sakon Nakhon 47000, Thailand*
5 *Biodiversity and Utilization Research Unit, Center of Excellence in Modern Agriculture, Sakon Nakhon Rajabhat University, Sakon Nakhon 47000, Thailand*

https://zoobank.org/878BA02C-D70D-4B43-9F6D-0FAD25979917

Corresponding author: Ruttapon Srisonchai (ruttasr@kku.ac.th)

Academic editor: Luiz Felipe Iniesta ♦ **Received** 12 December 2024 ♦ **Accepted** 25 January 2025 ♦ **Published** 26 February 2025

Abstract

An examination of newly collected material from northeastern Thailand revealed three new millipede species in the genus *Enghoffosoma* Golovatch, 1993: *E. furca* **sp. nov.**, *E. parvispina* **sp. nov.**, and *E. rubellum* **sp. nov.** We utilized morphological evidence together with genetic analysis of the COI gene to validate species identification. Each of the new species has unique characteristics, particularly in the structure of the gonopodal solenophore, that easily distinguish them from other species in the genus. The interspecific *p*-distances calculated from 658-bp barcoding sequences between the new species and their congeners show ranges of 18.56% to 22.78% for *E. furca* **sp. nov.**, 15.09% to 21.25% for *E. parvispina* **sp. nov.**, and 15.09% to 22.37% for *E. rubellum* **sp. nov.**, supporting the morphological distinctions. Preliminary phylogenetic trees using Bayesian inference (BI) and maximum likelihood (ML) indicate that the genus *Enghoffosoma* is monophyletic, with two of the newly described species forming distinct clades. Our findings increase the total number of *Enghoffosoma* species to 16 (including six in Thailand) and underscore a greater diversity within the genus than previously known. Morphological illustrations of the new species, derived from SEM micrographs, and a distribution map of all known species are included.

Key Words

Biodiversity, identification, phylogeny, South-East Asia, taxonomy

Introduction

Currently, Thailand stands out as a significant hotspot for millipede diversity with a total of 282 species identified across various habitats. Notably, approximately 84% of these species are endemic, highlighting the unique biodiversity in the country's ecosystems. Among the families of millipede in the class Diplopoda, the family Paradoxosomatidae Daday, 1889 has long been recognized as the most species-rich group not only globally (1,600 species) but also in Thailand, comprising 106 out of the total 267 described species (Likhitrakarn et al. 2023).

Research on the systematics of several groups of millipedes has progressed rapidly in Thailand in recent years (Pimvichai et al. 2009, 2014; Likhitrakarn et al. 2010, 2011; Srisonchai et al. 2018, 2024). However, only a few genera of Paradoxosomatidae, such as *Desmoxytes* Chamberlin, 1923, *Gigaxytes* Srisonchai, Enghoff & Panha, 2018, *Nagaxytes* Srisonchai, Enghoff & Panha, 2018, *Siamaxytes* Srisonchai & Panha, 2024, and *Spinaxytes* Srisonchai et al., 2018,

Copyright *Benchapong, T. et al.* This is an open access article distributed under the terms of the Creative Commons Attribution License (CC BY 4.0), which permits unrestricted use, distribution, and reproduction in any medium, provided the original author and source are credited.

have been analyzed integratively (Srisonchai et al. 2024). Additionally, some paradoxosomatid genera occurring in the country (viz., *Orthomorpha* Bollman, 1893, *Antheromorpha* Jeekel, 1968, *Tylopus* Jeekel, 1968 and *Enghoffosoma* Golovatch, 1993), which exhibit a diverse range of morphological characteristics are lacking genetic analysis and still require systematic revision (Likhitrakarn et al. 2011).

The millipede genus *Enghoffosoma* Golovatch, 1993 is probably one of the most taxonomically diverse genera of Paradoxosomatidae in Asia, especially in South-East Asia (Likhitrakarn et al. 2014). The members of the genus are primarily distinguished based on gonopod characters in combination with other somatic features. To date, 13 species of *Enghoffosoma* have been described worldwide: one species in China, two species in Laos, one species in Myanmar, 6 species in Vietnam, and 3 species in Thailand (*E. bispinum* Likhitrakarn, Golovatch & Panha, 2014; *E. funda* Likhitrakarn, Golovatch & Panha, 2014; and *E. zebra* Likhitrakarn, Golovatch & Panha, 2014) (Golovatch 1993, 2011, 2016; Golovatch et al. 2016; Golovatch and Semenyuk 2018; Likhitrakarn et al. 2014; Nguyen and Golovatch 2016).

In the present study, we examined recently collected specimens of *Enghoffosoma* from the northeastern region of Thailand. These specimens appear to be geographically isolated from other species. Morphological evidence obtained from scanning electron micrographs and molecular data support the identification of three distinct morphotypes, which are described here as new species.

Materials and methods

Specimen collections and preservation

The specimens were collected by hand from the northeastern region of Thailand. Live animals were photographed in the field using a Canon EOS 90D digital camera equipped with a Canon EF-S 60 mm f/2.8 Macro USM lens. All specimens were placed in 10% ethanol for proper euthanization based on the procedure of the American Veterinary Medical Association (American Veterinary Medical Association 2020), and subsequently preserved in 70% ethanol for morphological examination, and 95% ethyl alcohol for DNA analysis.

The collecting sites (latitude, longitude, and elevation) were recorded by a Garmin GPSMAP 60CSx, and all exact coordinates were double-checked with Google Earth. The background image for the distribution map was taken from the website Elastic Terrain Map (http://elastic-terrain.xyz/) and altered with Adobe Photoshop CC2024.

This work was conducted under the approval of the Khon Kaen University's Animal Care and Use Committee (Protocol Reviews No. IACUC-KKU-70/67) and with permission to conduct research in protected areas (Department of National Parks, Wildlife and Plant Conservation; Protocols No. 23103 and 23104).

Morphological study

All specimens were studied under a Nikon SMZ445 stereo microscope and were measured with a TIGA 6x1/128 in a vernier caliper. For scanning electron micrographs, dissected body parts were mounted on aluminum stubs, air-dried, coated with gold at 30 mAmp for 240 seconds, and then studied under a JEOL, JSM-5410 LV microscope. After imaging, all specimens were removed from the stubs and preserved in ethanol in Eppendorf tubes for long-term preservation. The images were processed and edited with Adobe Photoshop CC2024 and line drawings were sketched in Adobe Illustrator 2018.

The species identification and morphological descriptions followed Golovatch (1993, 2011, 2016), Likhitrakarn et al. (2014), Golovatch and Semenyuk (2018), Nguyen and Golovatch (2016), and Srisonchai et al. (2023, 2024).

Abbreviations of somatic characters

cl claw of leg,
cx coxa of leg,
ep epiproct,
fe femur of leg,
hy hypoproct,
oz ozopore,
pfe prefemur of leg,
pk pleurosternal keel,
pof postfemur of leg,
pp paraproct,
sc sensory cones,
ta tarsus of leg,
ti tibia of leg,
vb ventral brushes.

Abbreviations of gonopod characters

a process a on solenophore,
ca cannula of gonopod,
cox coxa of gonopod,
fm femur,
ls lateral sulcus,
p process p on femur,
prf prefemur of gonopod,
sg seminal groove of gonopod,
sl solenomere of gonopod,
sp spatula-like process,
sph solenophore of gonopod,
sph-l small process located on base of solenophore, clearly seen in lateral view,
sph-m small process located on base of solenophore, clearly seen in mesal view.

Institutional abbreviations

CUMZ Chulalongkorn University Museum of Zoology, Bangkok, Thailand
MZKKU Khon Kaen University Museum of Zoology, Thailand (invertebrate collections)
NHM Natural History Museum, London, United Kingdom
NHMW Natural History Museum, Vienna, Austria
NHMD Natural History Museum of Denmark, University of Copenhagen, Denmark
ZFMK Zoological Research Museum A. Koenig, Leibniz Institute for Animal Biodiversity, Bonn, Germany

DNA extraction, amplification, sequencing and phylogenetic reconstruction

A total of 24 sequences were used for phylogenetic study, comprising 17 sequences from this study and 7 sequences available from GenBank (Suppl. material 1). Outgroups were selected based on the recent phylogenetic studied including *Antheromorpha festiva* (Brölemann, 1916), *Desmoxytes planata* (Pocock, 1895), *Orthomorpha setosa* (Attems, 1937), *Oxidus gracilis* (C.L. Koch, 1847) and *Tylopus roseiparaterga* Nguyen, 2012 (Nguyen et al. 2018; Likhitrakarn et al. 2019; Srisonchai et al. 2024). The new sequences have been submitted to GenBank, and their accession numbers are shown in Suppl. material 1 (PV031917–PV031933).

Genomic DNA was extracted from body rings and leg tissues using the NucleoSpin Tissue Kit. The COI gene was amplified via polymerase chain reactions (PCR) using the universal primers LCO1490 and HCO2198 — LCO-1490 (5′-GGT CAA CAA ATC ATA AAG ATA TTG G-3′) and HCO-2198 (5′-TAA ACT TCA GGG TGA CCA AAA AAT CA-3′) (Folmer et al. 1994). The PCR reaction was performed in a total volume of 40.0 µL, consisting of EmeraldAmp GT PCR Master Mix (16 µL), ddH_2O (12 µL), 8 µL primers (4 µL each), and 4.0 µL of DNA template. The annealing step was carried out at 43 °C for 1 minute, followed by an extension step at 72 °C for 2 minutes. PCR products were screened for successful amplification of COI fragments using 1% agarose gel electrophoresis with TBE 1X and were observed under UV trans-illumination. The resulting amplified products were sent for commercial sequencing at Bioneer Corporation, South Korea.

The DNA sequences were checked for errors by putting them into the same reading frame, translating into proteins, and all sequences were aligned using MEGA 11 (Tamura et al. 2021). The aligned data were subsequently analyzed with JModelTest2 on XSEDE (Darriba et al. 2012) through the CIPRES Gateway (Miller et al. 2010) to assess nucleotide evolution models and identify the best-fit substitution model.

The phylogenetic trees were reconstructed using, Bayesian inference (BI) and maximum likelihood (ML), through the online CIPRES Science Gateway (Miller et al. 2010). For the BI analysis, data were executed with KAKUSAN 4.0 (Tanabe 2011) to generate the original file, adjusting for the best-fit model (GTR+I+G). The analysis was then conducted in MrBayes on XSEDE 3.2.7a (Ronquist et al. 2012), using a Markov chain Monte Carlo (MCMC) approach for 30 million generations, running with 4 chains of MCMC and sampling every 1,000 generations. For ML analysis, an optimal tree was conducted by using IQ-Tree on XSEDE 2.3.2 (Minh et al. 2020) with the GTR+I+G substitution model and branch support was estimated using 1,000 bootstrap (BS) replicates. The visualizations of the ML and BI trees were accomplished in FigTree v. 1.4.4 (Rambaut 2018), and visually processed in Adobe Illustrator 2018. The evaluation of node robustness involves considering maximum likelihood bootstrap support values (BS) > 70% and Bayesian inference posterior probabilities (PP) > 0.95% as strong support (Hillis and Bull 1993; Huelsenbeck and Rannala 2004).

Uncorrected pairwise genetic distances (*p*-distances) were also calculated in MEGA 11.

Results

DNA sequences and phylogenetic tree

The COI sequence alignments consisted of 658 base pairs with 243 variable sites, 415 conserved sites, and 187 parsimony-informative sites. The range of percentual distances between outgroups (*A. festiva*, *D. planata*, *O. setosa*, *O. gracilis*, and *T. roseiparaterga*) and *Enghoffosoma* species was 17.82–30.85%. The range of interspecific distances within the genus *Enghoffosoma* was 15.09–22.78%. The interspecific distances between other *Enghoffosoma* species (vs the three new species) were 18.56–22.78% for *E. furca* sp. nov., 15.09–21.25% for *E. parvispina* sp. nov. and 15.09–22.37% for *E. rubellum* sp. nov. The largest intraspecific distance was found in *E. parvispina* with 1.88%. Additional information for genetic distances is provided in Suppl. material 2.

The Bayesian inference and maximum likelihood analyses based on the COI gene fragment resulted in the same topology for the ingroup (Fig. 1). The genus *Enghoffosoma* is monophyletic with high support (PP = 0.99, BS = 79). However, some deep nodes on trees had low statistical support which questions the reliability of the calculated relationships within the genus. The new species are recovered as monophyletic with strong support, with *E. parvispina* sp. nov. nested together with *E. rubellum* sp. nov. (PP = 1, BS = 67), while *E. furca* sp. nov., represented by only one terminal, was grouped together with *E. bispinum* (PP = 1.00, BS = 73).

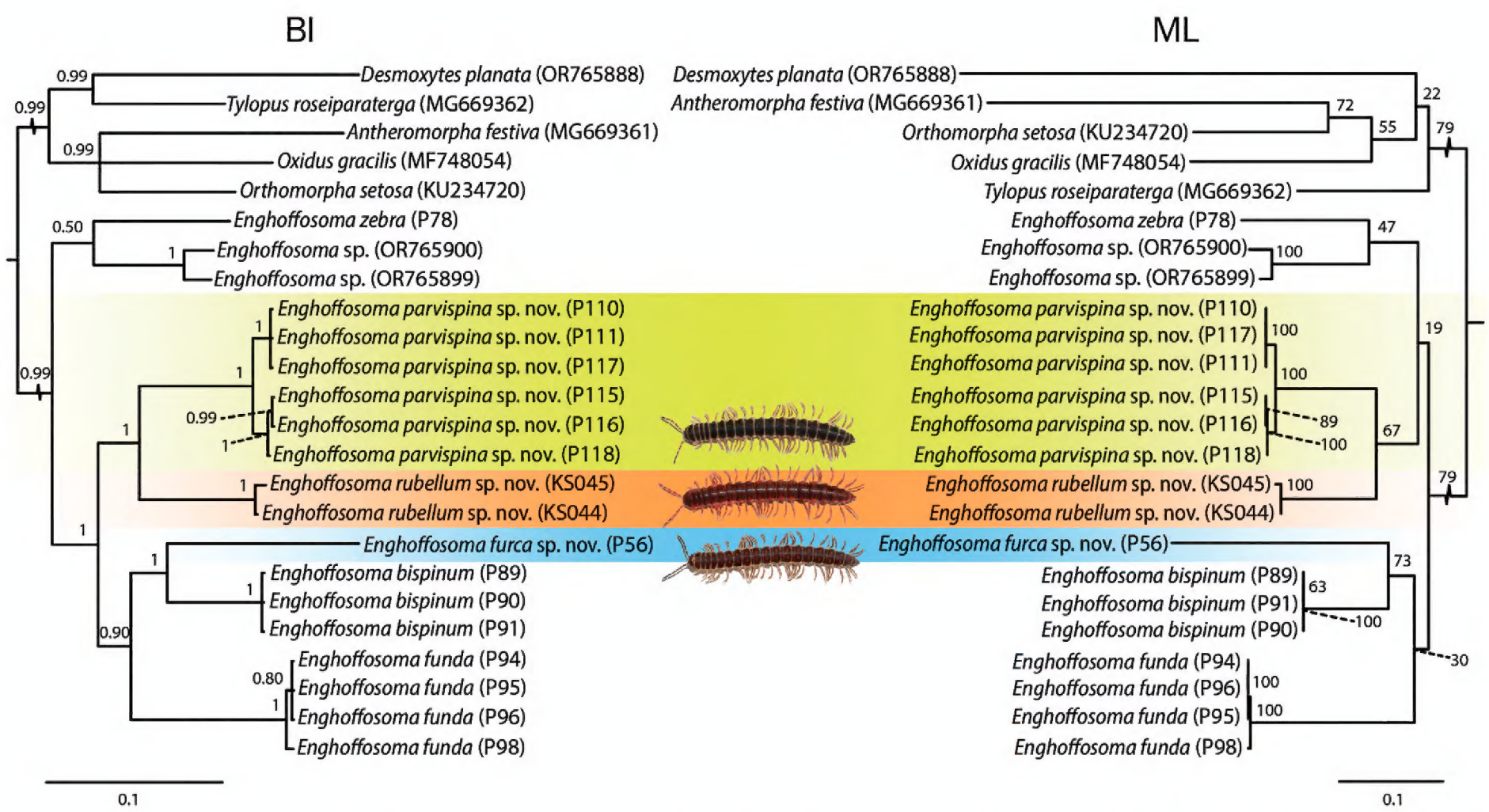

Figure 1. Phylogenetic tree of COI gene fragment based on Bayesian Inference (BI) and maximum likelihood (ML). Nodal numbers refer to Bayesian posterior probabilities (PP) from BI and bootstrap support (BS) from ML. Different colors represent three new species (*Enghoffosoma furca* sp. nov., *Enghoffosoma parvispina* sp. nov. and *Enghoffosoma rubellum* sp. nov.), corresponding to the live photographs. Scale bar indicates substitutions per site.

Systematics

Class Diplopoda de Blainville in Gervais, 1844
Order Polydesmida Pocock, 1887
Family Paradoxosomatidae Daday, 1889
Subfamily Paradoxosomatinae Daday, 1889
Tribe Paradoxosomatini Daday, 1889

Genus *Enghoffosoma* Golovatch, 1993

Enghoffosoma Golovatch, 1993: 8.

Enghoffosoma — Golovatch, 2011: 262; Nguyen and Sierwald 2013: 1258; Likhitrakarn et al., 2014: 492; Nguyen and Golovatch 2016: 152; Golovatch and Semenyuk 2018: 7; Likhitrakarn et al. 2023: 74.

Diagnosis. *Enghoffosoma* can be differentiated from the other seven genera within the tribe Paradoxosomatini by the following combination of characteristics: paraterga conspicuous as short keels; pleurosternal keel present on rings 2–17; gonopod telopodite suberect, typically branched, with a very long and slender solenophore; solenomere also very long; femur often bearing a distal process; a distinct demarcation between the femur and the postfemoral portion; solenophore frequently featuring process(es) or lobe(s) near its base. *Enghoffosoma* is distinguished from *Ciliciosoma* Verhoeff, 1940, *Strongylosoma* Brandt, 1883, and *Substrongylosoma* Golovatch, 1984 by the presence of a conspicuous demarcation between the femur and the postfemoral part of the gonopod. The gonopod telopodite in *Enghoffosoma* is branched, which contrasts with *Haplogonomorpha* Mršić, 1996, whose species lack an apical branch. *Enghoffosoma* is separated from *Lohmanderodesmus* Schubart, 1934 and *Stosatea* Gray, 1843 by the typically long and slender solenophore in *Enghoffosoma* compared to the stout lobe in *Lohmanderodesmus* and the broad lamella in *Stosatea*. *Enghoffosoma* differs from *Tetrarthrosoma* Verhoeff, 1898 in having a distal process on the femur and a solenophore that branches into 2 or 3 processes.

Type-species. *Sundanina spinipleura* Carl, 1941.

List of Enghoffosoma species in Thailand. 1) *E. bispinum* Likhitrakarn, Golovatch & Panha, 2014. 2) *E. funda* Likhitrakarn, Golovatch & Panha, 2014. 3) *E. furca* sp. nov. 4) *E. parvispina* sp. nov. 5) *E. rubellum* sp. nov. 6) *E. zebra* Likhitrakarn, Golovatch & Panha, 2014.

Enghoffosoma bispinum Likhitrakarn, Golovatch & Panha, 2014

Enghoffosoma bispinum Likhitrakarn, Golovatch & Panha, 2014 in Likhitrakarn et al. 2014: 508.

Enghoffosoma bispinum — Nguyen & Golovatch, 2016: 151; Likhitrakarn et al. 2023: 74; Srisonchai et al. 2024: 4.

Material examined. Thailand • 3 ♂ 2 ♀ (MZKKU); Rayong Province, Mueang Rayong District, Khao Yai Chum Temple; 12°39'23.7"N, 101°26'47.8"E; 21 July 2024; R. Srisonchai and T. Benchapong leg.

Distribution and habitat. *E. bispinum* is currently known from only two locations in Rayong Province, situated just 10 km apart. All newly collected specimens were observed walking on the ground, with some found on thin layers of leaf litter.

Enghoffosoma funda Likhitrakarn, Golovatch & Panha, 2014

Enghoffosoma funda Likhitrakarn, Golovatch & Panha, 2014 in Likhitrakarn et al. 2014: 505.

Enghoffosoma funda — Nguyen & Golovatch, 2016: 151; Likhitrakarn et al. 2023: 74.

Material examined. Thailand • 15 ♂ 8 ♀ (MZKKU); Sisaket Province, Kantharalak District, Sisaket Nature Resources Environment Office # 6; 14°39'19.4"N, 104°37'34.4"E; 5 October 2024; T. Benchapong leg. • 25 ♂ 23 ♀ (MZKKU); Sisaket Province, Kantharalak District, Ban Kae Monastery; 14°41'13.8"N, 104°37'10.1"E; 5 October 2024; T. Benchapong leg.

Distribution and habitat. This species is restricted to a small area within the dry deciduous forests of Sisaket Province. The type locality and its surrounding area are characterized by sandstone habitats. A recent visit to the type locality confirmed the presence of several topotypic specimens, observed on humid ground covered with a thin layer of leaf litter.

Enghoffosoma furca Benchapong & Srisonchai, sp. nov.

https://zoobank.org/8EDBCF72-F232-4FAB-91BD-AE721F6987BD

Figs 2–5

Material examined. ***Holotype*:** Thailand • ♂ (MZKKU-MYR0007); Chaiyaphum Province, Phakdee Chumphon District, Thum Kaeo Monastery, on forest floor; 405 m a.s.l.; 15°58'27.2"N, 101°24'36.5"E; 3 September 2023; R. Srisonchai and T. Benchapong leg.

***Paratypes*:** Thailand • 7 ♂♂, 5 ♀♀ (MZKKU-MYR0008); same data as holotype • ♂ (CUMZ-MYR0034); same data as for holotype • ♂ (NHM); same data as for holotype • ♂ (NHMD); same data as for holotype • ♂ (NHMW), same data as for holotype • ♂ (ZFMK-MYR14168); same data as for holotype.

Other materials. Thailand • ♂ broken specimen (MZKKU); same data as holotype.

Etymology. The specific name is a Latin noun in apposition and refers to the two-pronged fork solenomere.

Diagnosis. Distal region of femoral part of gonopod without process, and tip of solenomere forklike (Fig. 5A–E, J–H). Similar in these respects to *E. triangulare* Nguyen & Golovatch, 2016 (Fig. 15G), but the new species differs from it by having tip of largest process *in situ* directed posteriad (vs mesad) (Figs 5D, 14D, G, 15D, G). Genetically distant from the other *Enghoffosoma* species by 18.56–22.78% of COI sequences.

Description. Holotype: length 30.4 mm, height of midbody 3.5 mm, width of midbody prozonum and metazonum 3.0 and 3.5 mm, respectively. Males: length 27.5–29.4 mm, height of midbody 3.3–3.5 mm, width of midbody prozona and metazona 3.1–3.2 and 3.6–3.7 mm, respectively. Females: length 28.8–32.9 mm, height of midbody 3.5 mm, width of midbody prozona and metazona 3.5–3.6 and 4.0–4.1 mm, respectively. Width of head < collum = ring 2 = 3= 4 < 5–13 (male); head < ring 2 = 3 < 4 < collum < 5–13 (female), thereafter gradually tapering towards telson.

Coloration (Fig. 2A–C): Color of specimens in life predominantly dark brown to blackish brown. Head, antenna, collum, metaterga and epiproct dark brown to blackish brown (except pale brown tip of epiproct). Anterior part of collum and intermediate part of metaterga with pale brown patches. Paraterga and sterna yellowish white. Surface below paraterga and legs brown. A few basal podomeres of leg pale brown. Coloration in alcohol after one year of preservation faded to dark brown.

Head and clypeolabral region (Figs 3K, 4A, C): Vertex bare; with a shallow and conspicuous epicranial suture. Frons sparsely setose. Clypeus and labrum normal.

Antennae (Figs 3G, K, 4A, B): Short; covered by long and dense setae; reaching backward to ring 3 (♂) or 2 (♀). In length, antennomeres 6>2=3=4=5>1=7. Antennomeres 5–7 slightly clavate; each with a group of sensilla basiconica distally. With four apical cones.

Collum (Fig. 3A, D): Broad and wide. With two transverse rows of inconspicuous setae; 2+2 in anterior position and 1+1 ca. at midlength of collum. Paraterga of collum poorly developed (= obtuse tip).

Tegument (Figs 3A–F, H, 4K, H): With microspinulation, velvetlike. Prozona, metazona, paraterga and surface below paraterga microspinulate. Prozona on lateral side of body finely shagreened.

Metaterga (Figs 3H, I, 4L): Metatergum 2 with one transverse row of setae (mostly inconspicuous and broken off), 2+2 in anterior position. Metaterga 3–19 with one transverse row of setae, 1+1 in anterior position. Stricture between prozona and metazona striolate, shallow and narrow. Axial line and transverse sulcus missing.

Limbus (Fig. 4J): Limbus of midbody ring conspicuous; with rows of very long filaments, fused, arranged anteroposteriorly; margin finely spiculate; surface in front of limbus with a low ridge.

Paraterga (Figs 3H, I, 4G): Quite short, stout and small. Paraterga 2–4 short and thin. Paraterga 5–17 stouter and larger than others. The following paraterga slightly reduced in size and gradually tapering toward telson. Lateral margin without incision. Posterior corner rounded, directed caudad. Ozopores conspicuous, small, oval; present on rings 5, 7, 9, 10, 12, 13, 15–19; visible in lateral view; located near tip of paraterga.

Pleurosternal keels (Figs 3D–F, 4D): Well-developed, conspicuous; slightly curved. Keels on rings 2–4 small; rings 2–8 crestlike, with a sharp caudal tooth posteriorly; gradually reduced to small caudal tooth in rings 9–17; absent in rings 18 and 19.

Telson (Fig. 3J, L, M, N): Preanal ring (epiproct) quite slender; coniform in dorsal view; lateral setiferous tubercles and apical tubercles inconspicuous; tip truncate; with four spinnerets arranged at the corner, each located inside a shallow depression and surrounded by a crownlike collar. Paraprocts simple, slightly convex. Hypoproct subtriangular; with inconspicuous setiferous tubercles.

Sterna (Fig. 4E, F): Sparsely setose; cross-impressions shallow; posteriorly with a small tubercle near each

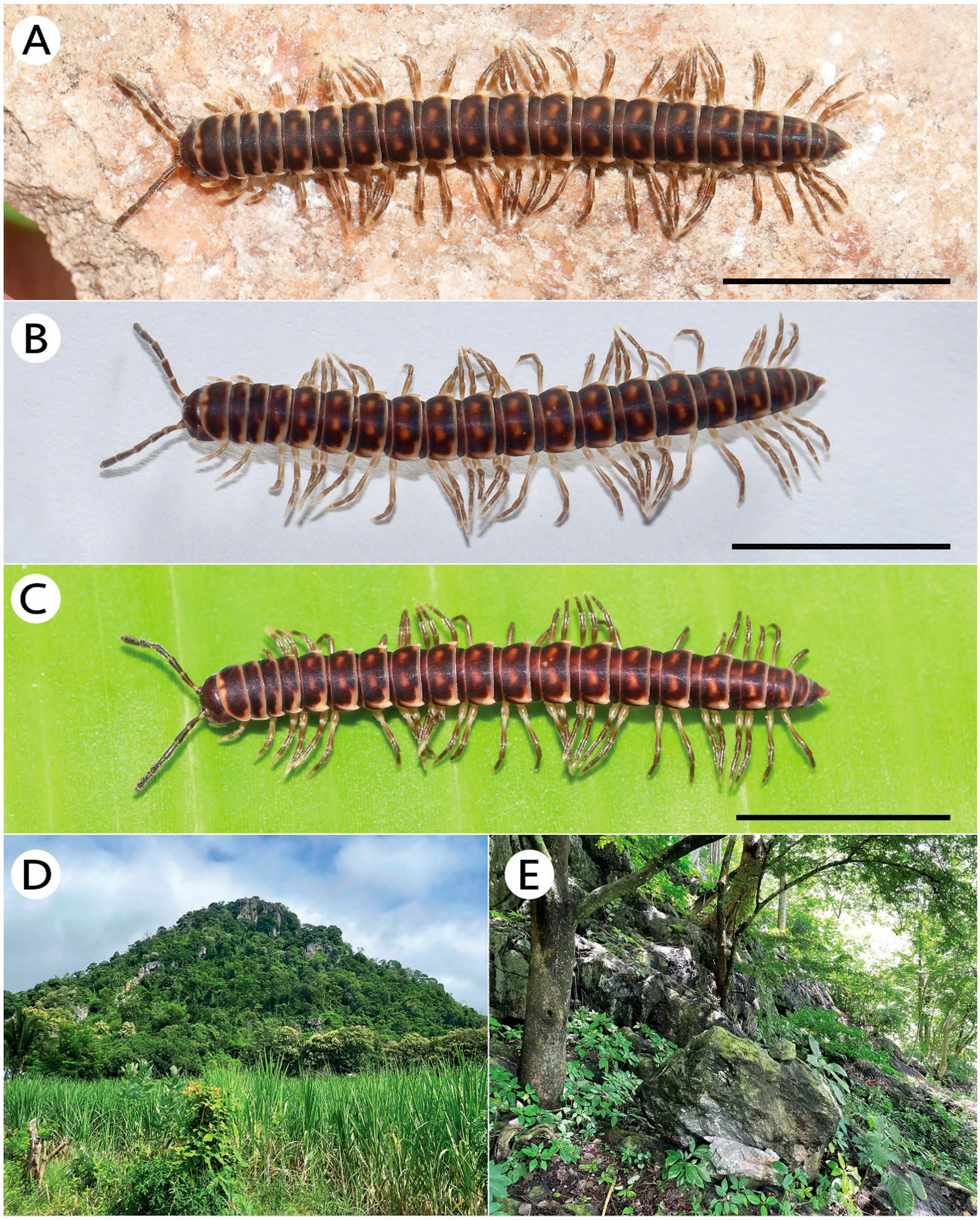

Figure 2. Live photographs of *Enghoffosoma furca* sp. nov. and habitat. **A–C.** Male paratype from type locality; **D, E.** Limestone habitat. Scale bars: 10 mm.

coxa. Sternal lobe between male coxae 4, large, subtrapeziform; tip truncate; with two pores.

Legs (Fig. 4M–O): Moderately long, slender, densely setose; length of midbody leg ca. 3.9–4.6 mm in both sexes; about 1.3–1.4 times (♂) or 1.1 times (♀) as long as midbody height. Prefemur slightly swollen basally. In length, femur > tibia > postfemur = prefemur > tarsus > coxa (♂). Distoventral part of tibia and tarsus of legs 1–10 in male with ventral brushes. Claw quite long, slender, pointed. Adenostyles in male absent.

Gonopods (Fig. 5): Coxa (cox) large; with a distoanterior group of setae. Cannula (ca) long and slender. Te-

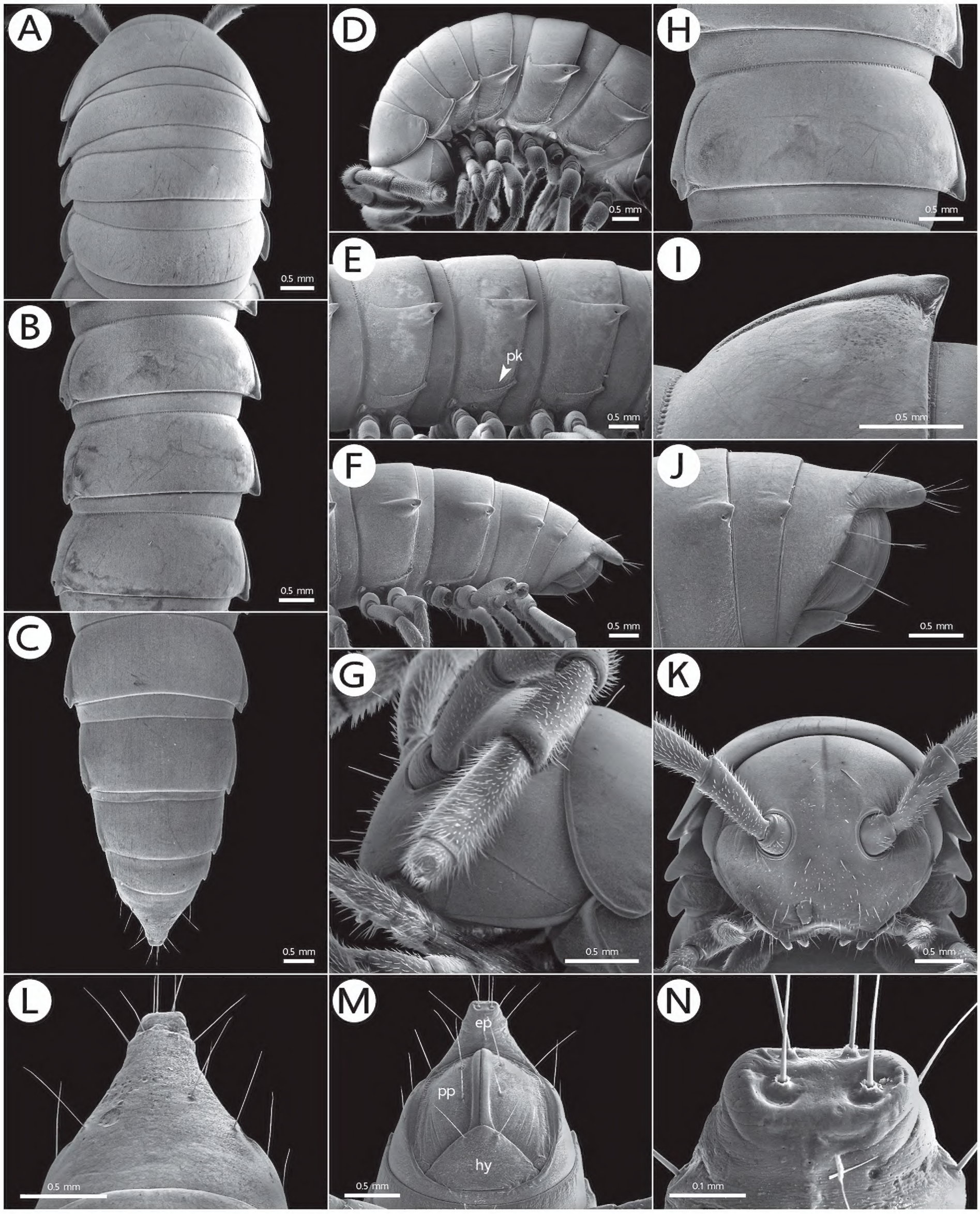

Figure 3. Scanning electron micrographs of *Enghoffosoma furca* sp. nov., male paratype (MZKKU-MYR0008). **A, D.** Anterior body part; **B, E.** Body rings 8–10; **C, F.** Posteriormost body rings and telson; **G.** Head and antenna; **H.** Body ring 10; **I.** Paraterga of ring 10; **J.** Telson; **K.** Head; **L–N.** Telson. **A–C, H, I, L.** Dorsal view; **D–F, G, J.** Lateral view. Abbreviations: ep = epiproct; hy = hypoproct; pk = pleurosternal keel; pp = paraproct.

lopodite long and slender; forming a 90° angle with coxa. Prefemur (prf) densely setose; about 1/2 as long as femur. Femur (fm) quite long and slender; without process distally. Seminal groove (sg) running entirely on mesal surface of femur. Lateral sulcus (ls) deep and conspicuous (Fig. 5B). Mesal sulcus inconspicuous. Postfemoral part inconspicuous. Solenophore (sph) well-developed; slightly broad; partly wrapped around solenomere; basomesally

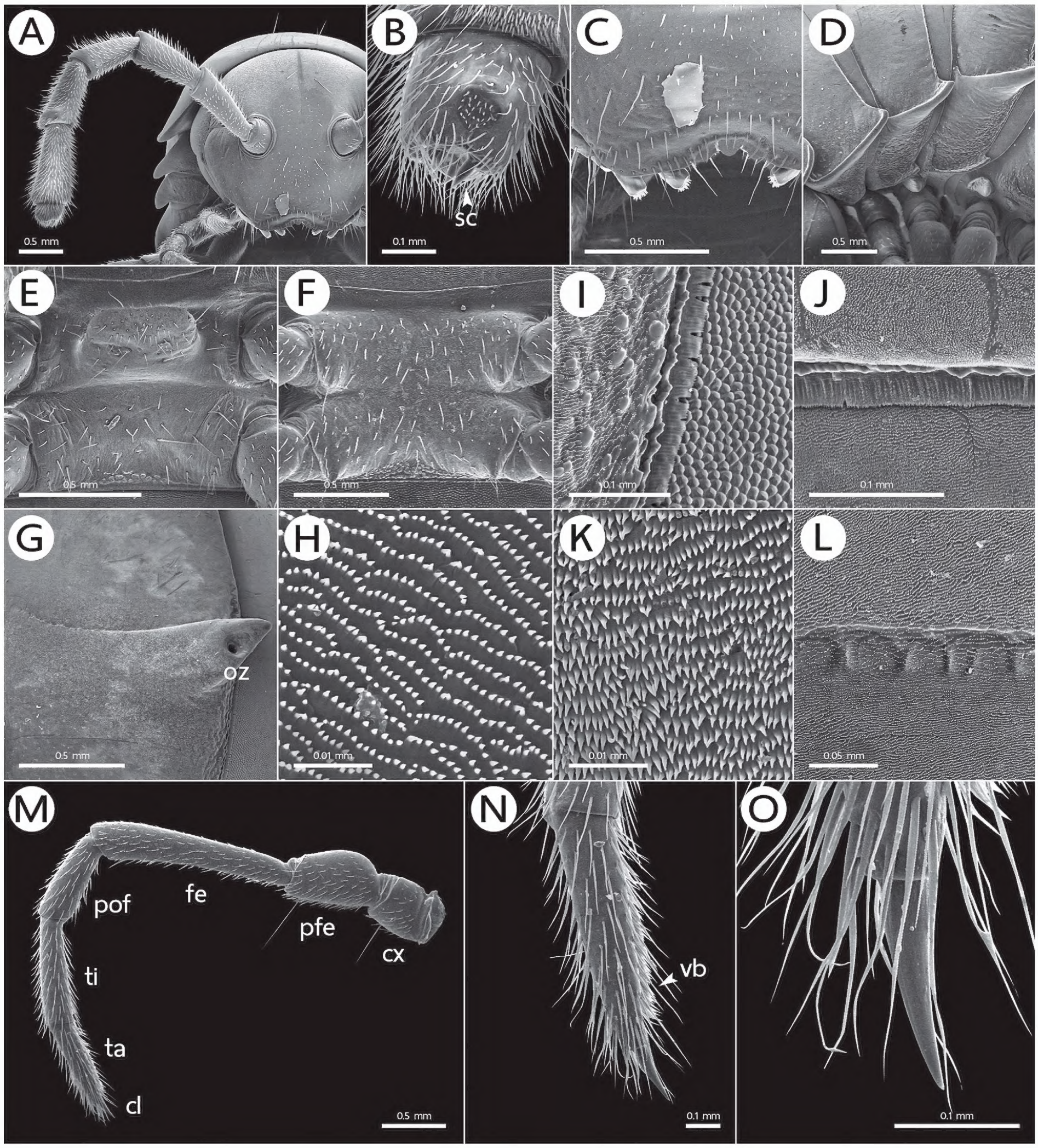

Figure 4. Scanning electron micrographs of *Enghoffosoma furca* sp. nov., male paratype (MZKKU-MYR0008). **A.** Head and antenna; **B.** Antennomeres 7 and 8; **C.** Clypeus, labrum and tip of gnathochilarium; **D.** Pleurosternal keels on rings 2–4; **E.** Sternal lobe between male coxae 4; **F.** Sternum of ring 10; **G.** Ozopore on paraterga of ring 10; **H.** Surface below paraterga of ring 10; **I, J.** Surface and limbus between rings 10 and 11, lateral and dorsal views; **K.** Surface of prozona of ring 10; **L.** Stricture between prozona and metazona of ring 10; **M.** Male right leg of ring 10; **N.** Ventral brushes on male tarsus; **O.** Claw. Abbreviations: cx = coxa; cl = claw; fe = femur; oz = ozopore; pfe = prefemur; pof = postfemur; sc = sensory cones; ta = tarsus; ti = tibia; vb = ventral brushes.

with three processes (two small and one large), tip of the large one *in situ* directed posteriad (Fig. 5D). Solenomere (sl) long; twisted; distally forklike, branching into two processes of the same length, with only the axial one having seminal groove running along it.

Distribution and habitat (Fig. 2D, E). Known only from the type locality in Chaiyaphum Province. All individuals were found walking on the ground among leaf litter in limestone forest habitat.

Remarks. In general appearance, *E. furca* sp. nov. is morphologically similar to *E. anchoriforme* Likhitrakarn et al., 2014 and *E. lanceolatum* Likhitrakarn et al., 2014 by showing dark brown color and with a small pale brown patch on each side of metaterga in both sexes (Fig. 2A–C).

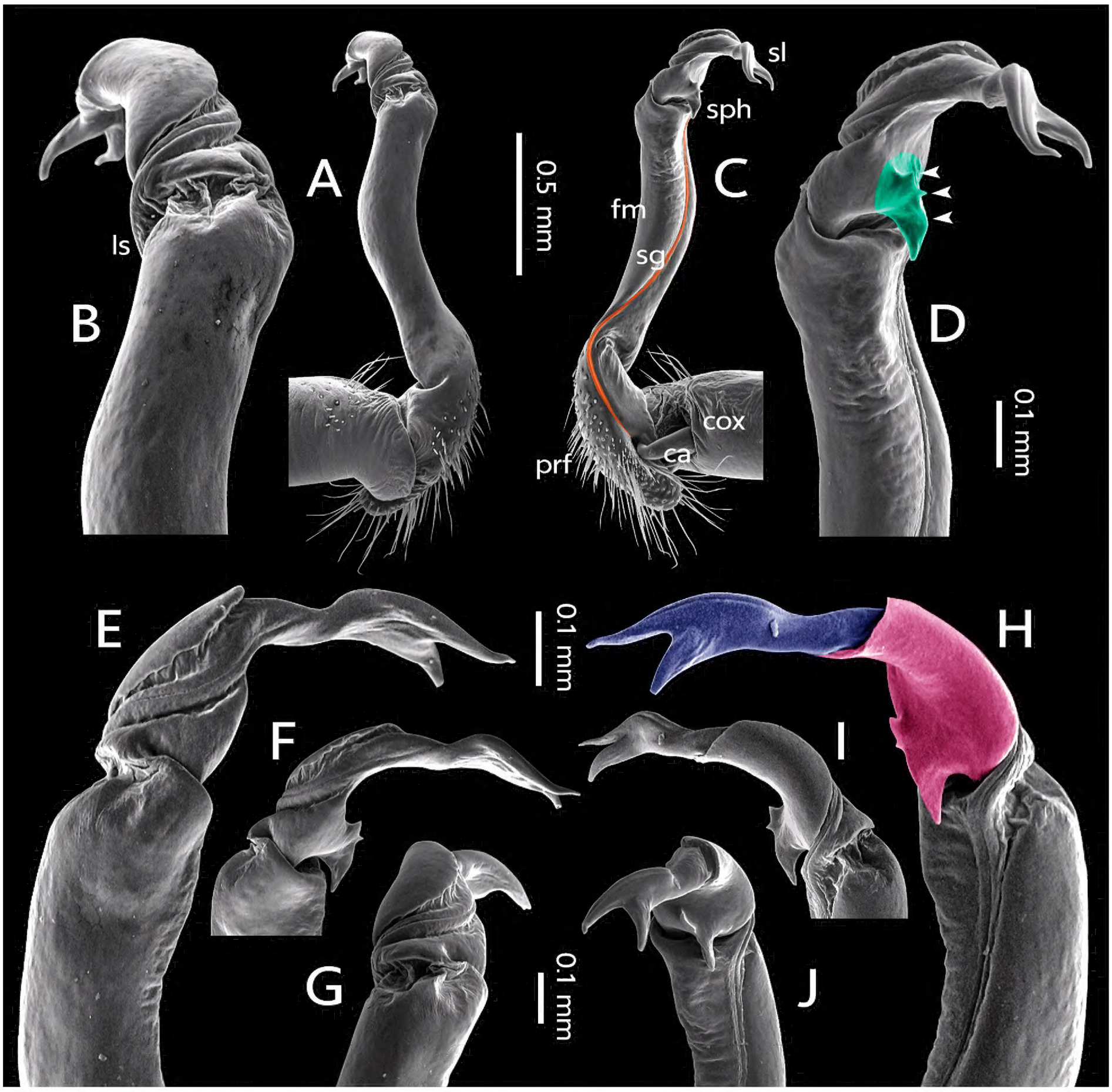

Figure 5. Scanning electron micrographs of *Enghoffosoma furca* sp. nov., right gonopod, male paratype (MZKKU-MYR0008). **A, B.** Lateral view; **C, D.** Mesal view (white arrows point to processes); **E.** Ventral view; **F, G.** Subventral view; **H.** Dorsal view; **I, J.** Subdorsal views. Colors: orange = seminal groove (sg); navy blue = solenomere (sl); pink = solenophore (sph); cyan = three processes. Abbreviations: cox = coxa; ca = cannula; fm = femur; ls = lateral sulcus; prf = prefemur; sg = seminal groove; sl = solenomere; sph = solenophore.

Enghoffosoma parvispina Benchapong & Srisonchai, sp. nov.

https://zoobank.org/D81AF0FC-7232-4766-9469-2F5BD78FEB6C

Figs 6–9

Material examined. ***Holotype*:** Thailand • ♂ (MZKKU-MYR0009); Ubon Ratchathani Province, Khong Chiam District, Tham Heo Sin Chai Temple, on forest floor; 130 m a.s.l.; 15°18'31.2"N, 105°29'07.6"E; 23 June 2024; R. Srisonchai and T. Benchapong leg.

***Paratypes*:** Thailand • 15 ♂♂, 15 ♀♀ (MZKKU-MYR0010); same data as for holotype • ♂, ♀ (CUMZ-MYR0035); same data as for holotype • ♂, ♀ (NHM); same data as for holotype • ♂, ♀ (NHMD); same data as for holotype • ♂, ♀ (NHMW), same data as for holotype • ♂ (ZFMK-MYR14170) ♀ (ZFMK-MYR14169); same data as for holotype.

Other materials. Thailand • 56 ♂♂, 4 ♀♀; same data as for holotype • ♂ (MZKKU); Ubon Ratchathani Province, Khong Chiam District, Thung Na Muang Waterfall, on forest floor; 130 m a.s.l.; 15°31'58"N, 105°35'48"E; 2 Jun. 2022; R. Srisonchai and T. Benchapong leg. • 8 ♂♂, 8 ♀♀ (MZKKU); Ubon Ratchathani Province, Khong Chiam District, Soi Sawan Waterfall, on forest floor; 240 m a.s.l.; 15°27'40"N, 105°34'39"E; 15 Jun. 2022; R. Srisonchai and T. Benchapong leg.; MZKKU • 15 ♂♂, 13 ♀♀ (MZKKU); Ubon Ratchathani Province, Khong Chiam District, Pha Taem National Park, on forest floor;

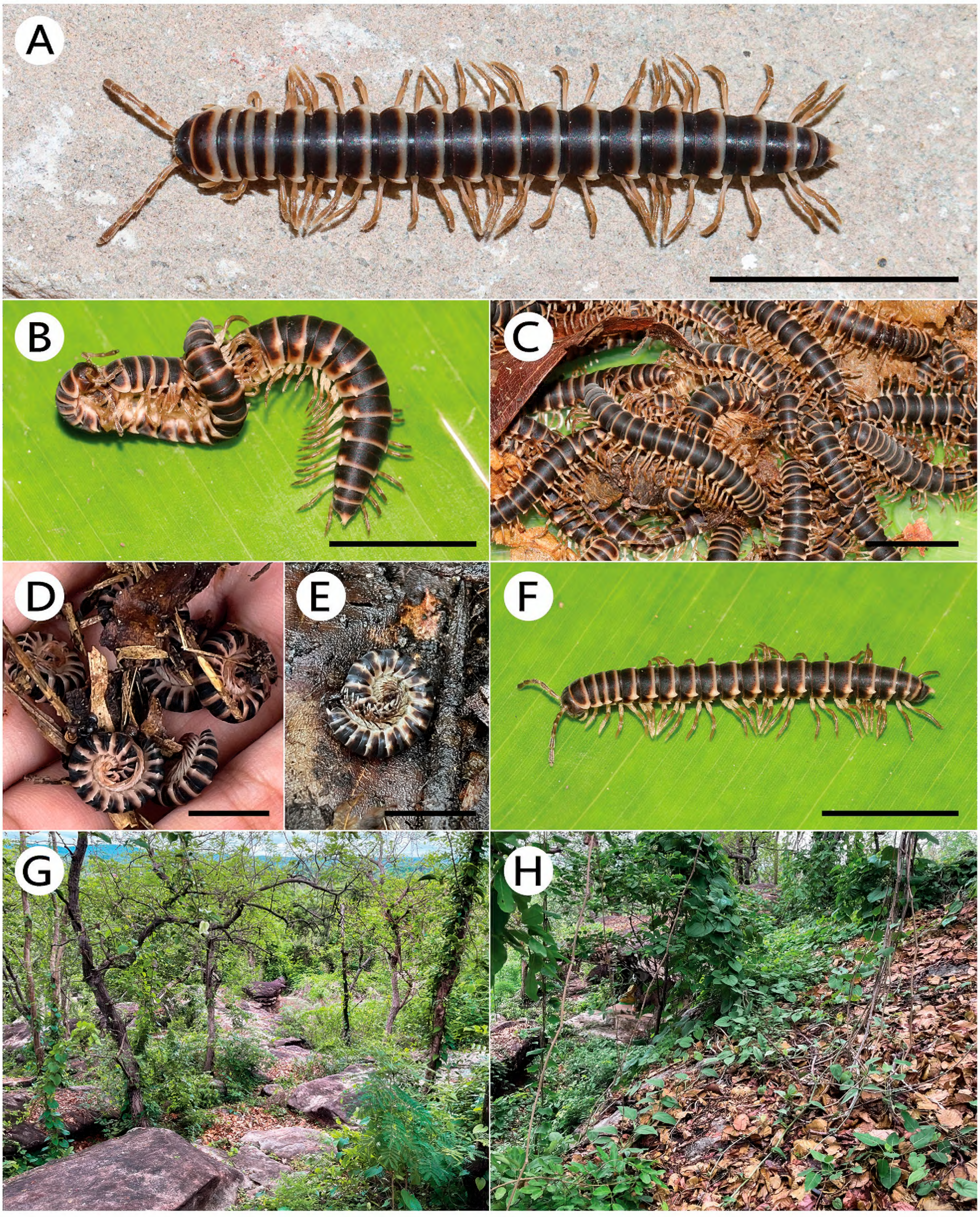

Figure 6. Live photographs of *Enghoffosoma parvispina* sp. nov. and habitat. **A–F, D.** Paratypes; **G, H.** Sandstone habitat. Scale bars: 10 mm.

200 m a.s.l.; 15°23'56.8"N, 105°30'29.8"E; 24 May. 2022; N. Likhitrakarn and R. Srisonchai leg. • 4 ♂♂, ♀ (MZKKU); Ubon Ratchathani Province, Khong Chiam District, Pha Taem National Park, on forest floor; 200 m a.s.l.; 15°23'56.8"N, 105°30'29.8"E; 23 June 2024; R. Srisonchai and T. Benchapong leg. • 2 ♀♀ (MZKKU); Ubon Ratchathani Province, Khong Chiam District, Khong Chiam Police Station, on forest floor; 90 m a.s.l.; 15°23'56.8"N, 105°30'29.8"E; 24 May 2022; N. Likhitrakarn and R. Srisonchai leg. • 4 ♂♂, 3 ♀♀ (MZKKU); Ubon Ratchathani Province, Khong Chiam District, Peerada Hug Moon, on forest floor; 100 m a.s.l.; 15°18'53.7"N, 105°29'59.1"E; 24 June 2024; R. Srisonchai and T. Benchapong leg.

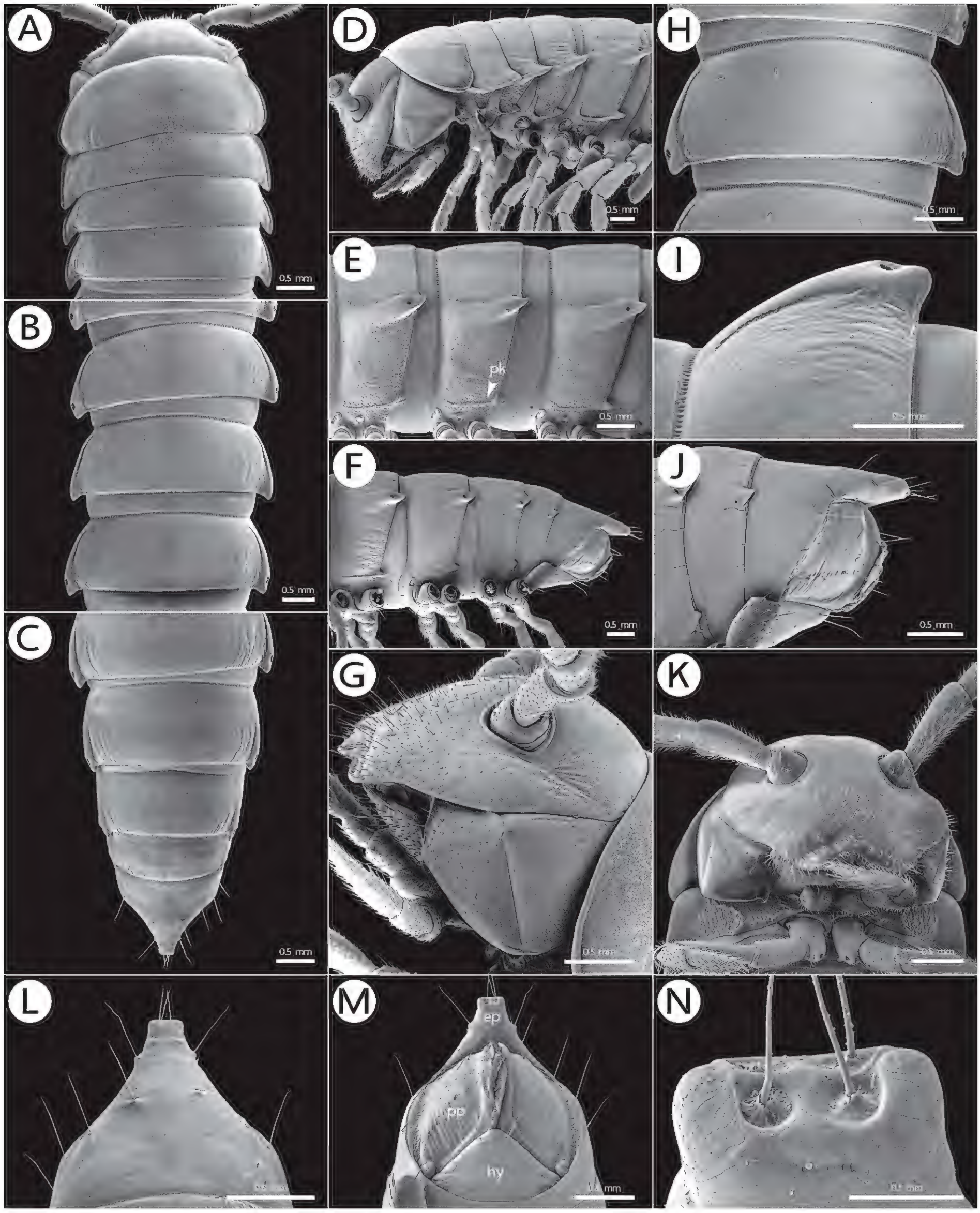

Figure 7. Scanning electron micrographs of *Enghoffosoma parvispina* sp. nov., male paratype (MZKKU-MYR0010). **A, D.** Anterior body part; **B, E.** Body rings 8–10; **C, F.** Posteriormost body rings and telson; **G.** Head and antenna; **H.** Body ring 10; **I.** Paraterga of ring 10; **J.** Telson; **K.** Head; **L–N.** Telson. **A–C, H, I, L.** Dorsal view; **D–F, G, J.** Lateral view. Abbreviations: ep = epiproct; hy = hypoproct; pk = pleurosternal keel; pp = paraproct.

Etymology. The specific name is a noun in apposition referring to a small process on the lateral base of the solenophore.

Diagnosis. Femoral part of gonopod with a long process (p) distally (Fig. 9D–G, I, J) and solenophore with two major lobes/processes (Fig. 9E). Similar in these

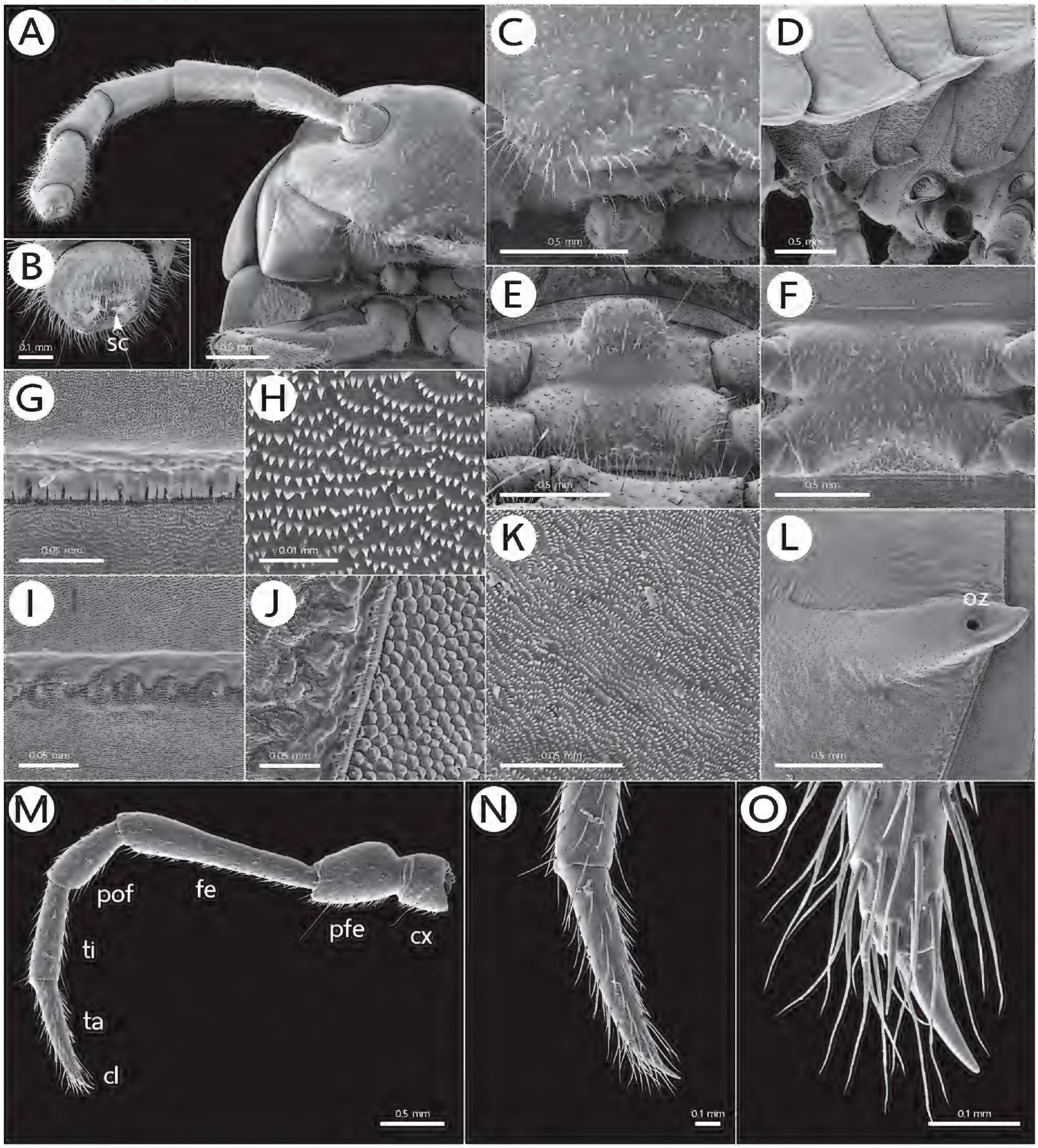

Figure 8. Scanning electron micrographs of *Enghoffosoma parvispina* sp. nov., male paratype (MZKKU-MYR0010). **A.** Head and antenna; **B.** Antennomeres 7 and 8; **C.** Clypeus, labrum and tip of gnathochilarium; **D.** Pleurosternal keels on rings 2–4; **E.** Sternal lobe between male coxae 4; **F.** Sternum of ring 10; **G, J.** Surface and limbus between rings 10 and 11, dorsal and lateral views; **H.** Surface of prozona of ring 10; **I.** Stricture between prozona and metazona of ring 10; **K.** Surface below paraterga of ring 10; **L.** Ozopore on paraterga of ring 10; **M.** Male right leg of ring 10; **N.** Tarsus; **O.** Claw. Abbreviations: cx = coxa; cl = claw; fe = femur; oz = ozopore; pfe = prefemur; pof = postfemur; sc = sensory cones; ta = tarsus; ti = tibia.

respects to *E. extraspinosum* Golovatch & Semenyuk, 2018 (Fig. 14B) and *E. rubellum* sp. nov. (Fig. 13). Differs from them by the presence of a small process (sph-l) at base of solenophore (Fig. 9B, E, I) and without ventral brushes on male legs 1–10. Genetically distant from other *Enghoffosoma* species by 15.09–21.25% of COI sequences.

Description. Holotype: length 28.5 mm, height of midbody 3.1 mm, width of midbody prozonum and metazonum 3.0 and 3.5 mm, respectively. Males: length 26.5–28.9 mm, height of midbody 2.7–3.2 mm, width of midbody prozona and metazona 2.7–3.1 and 3.3–3.6 mm, respectively. Females: length 28.1–30.6 mm, height of midbody 3.4–3.7 mm, width of midbody prozona and metazona 3.3–3.6 and

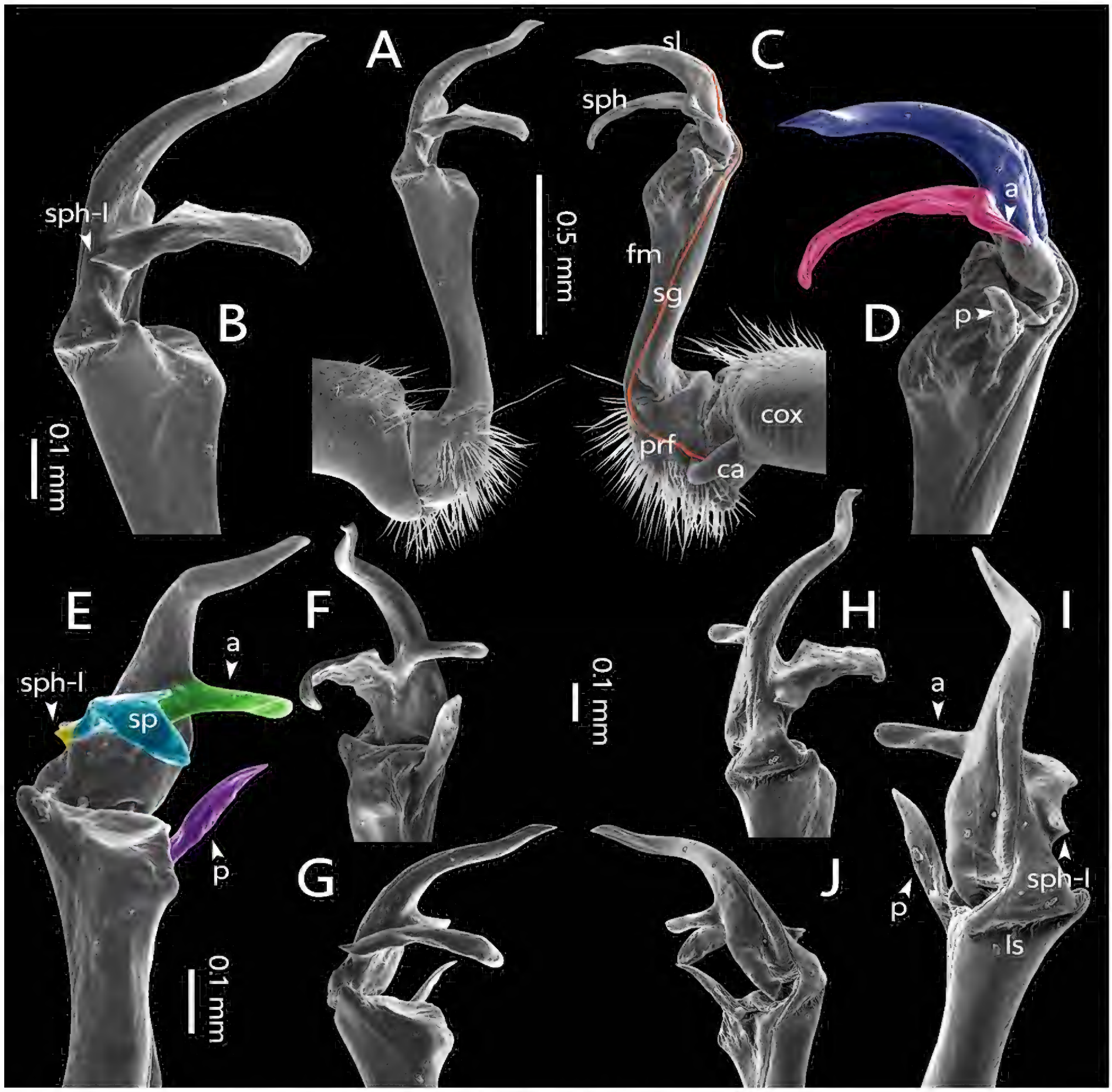

Figure 9. Scanning electron micrographs of *Enghoffosoma parvispina* sp. nov., holotype, right gonopod male paratype (MZK-KU-MYR0010). **A, B.** Lateral view; **C, D.** Mesal view; **E.** Ventral view; **F, G.** Subventral view; **H.** Dorsal view; **I, J.** Subdorsal view. Colors: green = process a (a); purple = process on femur (p); orange = seminal groove (sg); navy blue = solenomere (sl); pink = solenophore (sph); sky blue = spatula-like process (sp); yellow = lateral process on solenophore (sph-l). Abbreviations: a = process a; cox = coxa; ca = cannula; fm = femur; ls = lateral sulcus; p = process on femur; pfm = postfemur; prf = prefemur; sg = seminal groove; sl = solenomere; sph = solenophore; sph-l = lateral process on solenophore.

3.6–3.7 mm, respectively. Width of head < collum < ring 4 < 2 = 3 < 5–13 (male); head < ring 2 = 3 = 4 < collum < 5–15 (female), thereafter gradually tapering towards telson.

Coloration (Fig. 6A–F): Specimens in life brownish black or black. Head black. Antenna light brown. Collum, metaterga and surface below paraterga brownish black. Epiproct except the whitish tip, posterior part of collum and of metaterga brownish white. Paraterga, sterna and lower part of surface below paraterga and tip of epiproct white. Antenna and legs light brown; except a few basal podomeres whitish brown. Coloration in alcohol after two years of preservation changed to brownish black.

Head and clypeolabral region (Figs 7G, K, 8A, C): Vertex almost bare; epicranial suture conspicuous, shallow. Frons with sparse setae. Clypeus and labrum simple and normal.

Antennae (Fig. 8A, B): Quite short; densely setose; reaching backward to ring 4 (♂) or 3 (♀). In length, antennomeres 6>2=3=4=5>1=7. Antennomeres 5–7 clavate; each with a group of sensilla basiconica distally. With four apical cones.

Collum (Fig. 7A, D): Broad and wide. With two transverse rows of inconspicuous setae: 3+3 in anterior position and 1+1 in ca. at midlength of collum. Paraterga of collum poorly developed (= round tip).

Tegument (Figs 7A–F, H, 8H, K): With microspinulation. Prozona, metazona, paraterga and surface below paraterga microspinulate. Prozona on lateral side of body finely shagreened. Stricture between prozona and metazona striolate, quite deep and narrow.

Metaterga (Figs 9H, I, 8I): Metaterga 2–6 with one transverse row of setae (mostly inconspicuous and broken off), 3+3 in anterior position. Metaterga 7–19 with one transverse row of setae, 1+1 ca. at midlength of metaterga. Stricture between prozona and metazona striolate, shallow and narrow. Axial line and transverse sulcus missing.

Limbus (Fig. 8G): Limbus of midbody ring conspicuous; with rows of very long filaments, fused, arranged anteroposteriorly; margin finely spiculate; surface in front of limbus with a low ridge.

Paraterga (Figs 7H, I, 8L): Short, stout and small. Paraterga 2–4 short and thin. Paraterga 5–16 stouter and larger than others. The following paraterga slightly reduced in size and gradually tapering toward telson. No incision on lateral margin. Posterior corner obtuse, directed caudad. Ozopores conspicuous, small, oval; present on rings 5, 7, 9, 10, 12, 13, 15–19; visible in lateral view; located near tip of paraterga.

Pleurosternal keels (Figs 7D–F, 8D): Conspicuous. Rings 2–4 with small ridges; rings 2–8 crestlike, with a sharp caudal tooth posteriorly; increasingly reduced to small caudal tooth in rings 9–17; absent in rings 18 and 19.

Telson (Fig. 7J, L–N): Preanal ring (epiproct) quite slender, slightly attenuate near tip; lateral setiferous tubercles inconspicuous; apical tubercles a little swollen; tip truncate, sometimes concave; with four spinnerets arranged at the corner, each located inside a deep depression and surrounded by a crownlike collar. Paraprocts simple, slightly convex. Hypoproct subtriangular; with inconspicuous setiferous tubercles.

Sterna (Fig. 8E, F): Sparsely setose; cross-impressions shallow; posteriorly with a small tubercle near each coxa. Sternal lobe between male coxae 4, large, subtrapeziform; tip round; with two pores.

Legs (Fig. 8M–O): Moderately long, slender, densely setose; length of midbody leg ca. 4.1–4.6 mm in both sexes; about 1.4–1.5 times (♂) or 1.2–1.3 times (♀) as long as midbody height. Prefemur slightly swollen basally. In length, femur > tarsus > tibia > postfemur = prefemur > coxa (♂). Ventral brushes absent. Claw quite long, slender, pointed. Adenostyles in male absent.

Gonopods (Fig. 9): Coxa (cox) quite short and stout; with a distoanterior group of setae. Cannula (ca) long and slender. Telopodite long and slender; forming a 90° angle with coxa. Prefemur (prf) densely setose; about 1/2 as long as femur. Femur (fm) quite long and slender; distally with a long and sharp process (p), directed anteromesad. Seminal groove (sg) running entirely on mesal surface of femur. Lateral sulcus (ls) conspicuous, deep and wide. Mesal sulcus inconspicuous (Fig. 9L). Postfemoral part inconspicuous. Solenophore (sph) well-developed; consisting of three processes (two major and one small) (Fig. 9B, D). First process (sp) large and very long, spatula-like (Fig. 9D, E, I). Second process (a) smaller and shorter than the first one; located basomesally; tip *in situ* directed mesad (Fig. 9D, E, I). Third process (sph-l) smallest; spinelike; located at base of the first one; tip *in situ* directed ventrad (Fig. 9B, E, I). Solenomere (sl) very long and slender; slightly twisted.

Distribution and habitat (Fig. 6G, H). Based on extensive field surveys, this species inhabits sandstone habitats along the Mekong River in Ubon Ratchathani Province and, due to the proximity of the type locality near the Thai-Laos border, it may also occur in Laos and Cambodia.

Remarks. Based on gonopod solely, this species is very similar to *E. rubellum* sp. nov. It can be distinguished by the lateral small spine at base of solenophore (sph-l) (Fig. 9B, E, I).

Enghoffosoma rubellum Benchapong & Srisonchai, sp. nov.

https://zoobank.org/13D8D4AB-286A-490D-BD7F-90BBD677FC3D

Figs 10–13

Material examined. ***Holotype*:** Thailand • ♂ (MZKKU-MYR0011); Sakon Nakhon Province, Phu Phan District, Tham Si Kaeo Temple, on forest floor; 315 m a.s.l.; 16°55'18.5"N, 103°53'48.5"E; 22 August 2020; R. Chanabun, A. Aoonkum, R. Srisonchai and T. Benchapong leg.

***Paratypes*:** Thailand • ♂ (MZKKU-MYR0012); same data as for holotype • ♂ 4 ♀♀ (MZKKU-MYR00012); same data as for holotype; 13 Aug. 2022. • ♂ (CUMZ-MYR0036); same data as for holotype; 13 Aug. 2022 • ♂ (NHM); same data as for holotype; 13 Aug. 2022 • ♂ (NHMD); same data as for holotype; 13 Aug. 2022 • ♂ (NHMW), same data as for holotype; 13 Aug. 2022 • ♂ (ZFMK-MYR14171); same data as for holotype; 13 Aug. 2022.

Other materials. Thailand • 2 ♂♂, 3 ♀♀ (MZKKU); same data as for holotype • 9 broken ♂♂, 4 broken ♀♀ (MZKKU); same data as for holotype • ♂ (MZKKU); Sakon Nakhon Province, Phu Phan District, Tham Phrong Temple, on forest floor; 320 m a.s.l.; 16°49'18.3"N, 103°58'25.4"E; 22 August 2020; R. Srisonchai and T. Benchapong leg. • ♂ (MZKKU); Sakon Nakhon Province, Phu Phan District, Wiwekkaram Temple, on forest floor; 330 m a.s.l.; 16°51'03.0"N, 103°55'27.7"E; 22 August 2021; R. Srisonchai and T. Benchapong leg. • ♂ (MZKKU); Sakon Nakhon Province, Phu Phan District, Wiwekkaram Temple, on forest floor; 330 m a.s.l.; 16°51'03.0"N, 103°55'27.7"E; 13 August 2022.

Etymology. The specific name is an adjective and refers to the remarkable reddish brown body color of living specimens.

Diagnosis. Femoral part of gonopod with a long process (p) distally (Fig. 13D–I) and solenophore with two major lobes/processes (Fig. 13E). Similar in these respects to *E. extraspinosum* (Fig. 14B) and *E. parvispina* sp. nov. (Fig. 7). Differs from them by the presence of

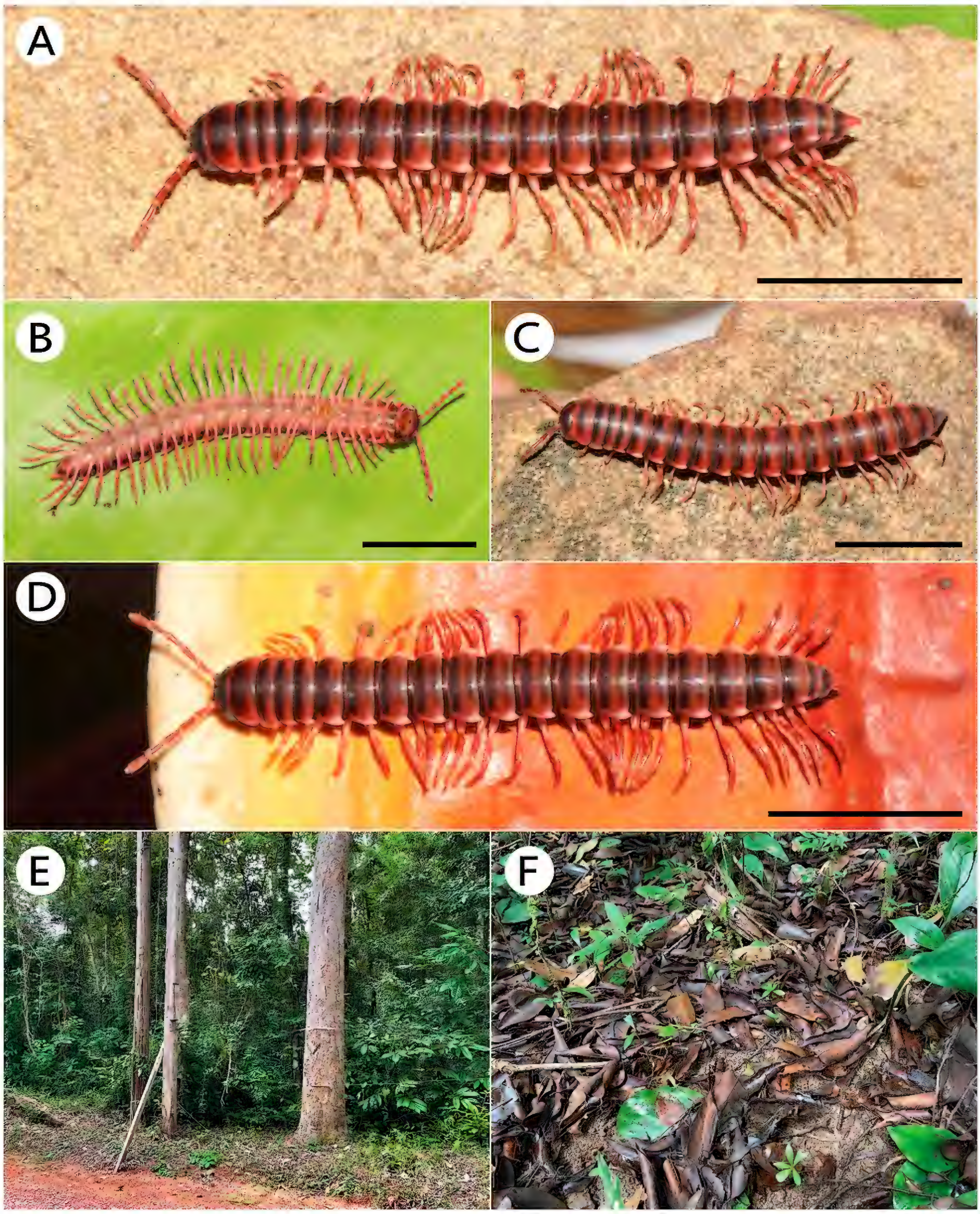

Figure 10. Live photographs of *Enghoffosoma rubellum* sp. nov. and habitat. **A–D.** Paratypes; **E, F.** Sandstone habitat. Scale bars: 10 mm.

a small process (process sph-m) at base of solenophore (Fig. 13C–F, H, I) and by having ventral brushes on male legs 1–10 (Fig. 12M). Genetically distant from other *Enghoffosoma* species by 15.09–22.37% of COI sequences.

Description. Holotype: length 25.7 mm, height of midbody 3.2 mm, width of midbody prozonum and metazonum 2.9 and 3.7 mm, respectively. Males: length 25.7–27.1 mm, height of midbody 3.2–3.6 mm, width of midbody prozona and metazona 2.7–3.1 and 3.3–3.6 mm, respectively. Females: length 28–35.4 mm, height of midbody 3.6–4.3 mm, width of midbody prozona and metazona 3.6–4.1 and 4.0–4.7 mm, respectively. Width of head < collum < ring 3 = 4 < 2 < 5–15 (male), head < collum < ring 2 = 3 = 4 < 5–15 (female), thereafter gently tapering towards telson.

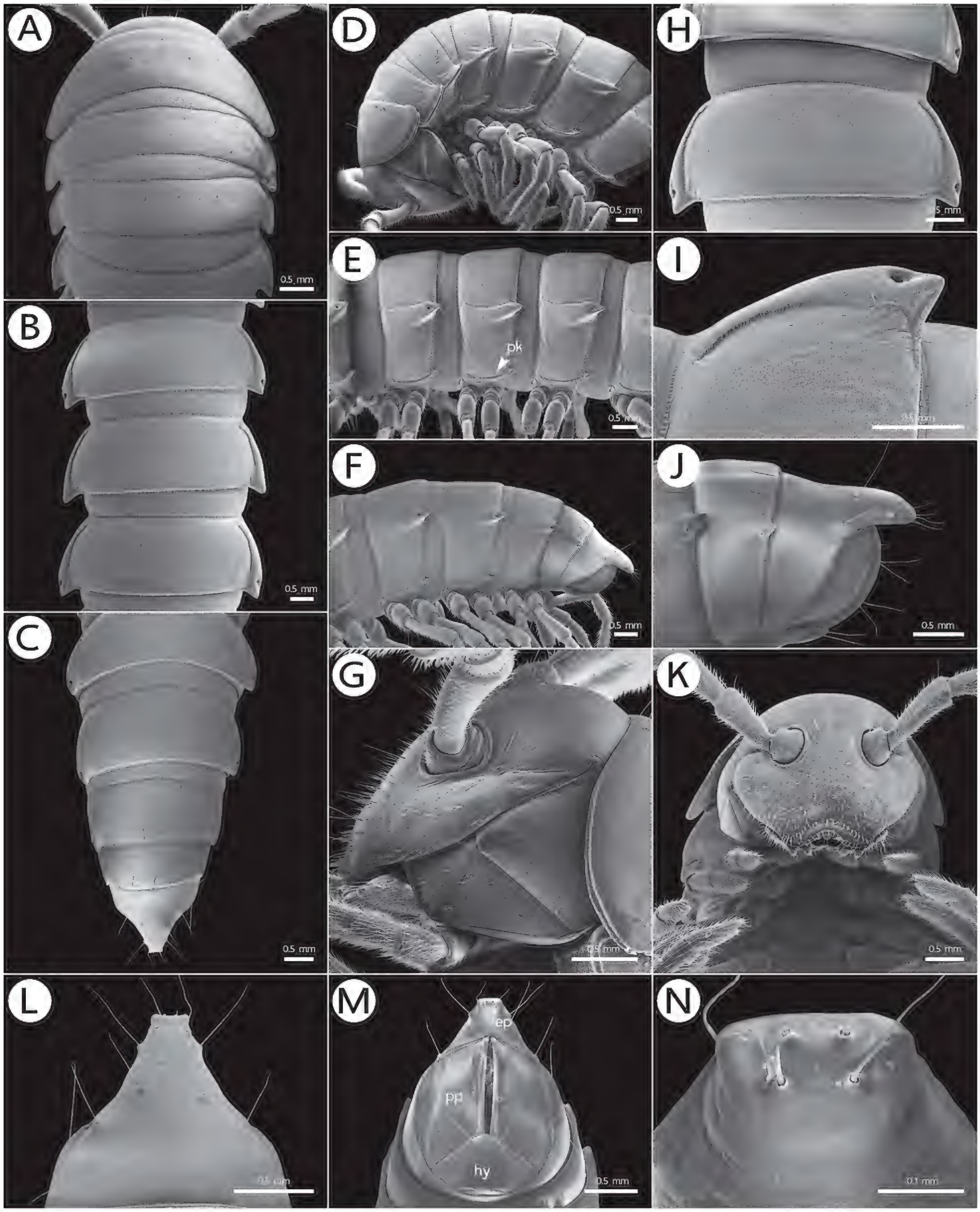

Figure 11. Scanning electron micrographs of *Enghoffosoma rubellum* sp. nov., male paratype (MZKKU-MYR0012). **A, D.** Anterior body part; **B, E.** Body rings 8–10; **C, F.** Posteriormost body rings and telson; **G.** Head and antenna; **H.** Body ring 10; **I.** Paraterga of ring 10; **J.** Telson; **K.** Head; **L–N.** Telson. **A–C, H, I, L.** Dorsal view; **D–F, G, J.** Lateral view. Abbreviations: ep = epiproct; hy = hypoproct; pk = pleurosternal keel; pp = paraproct.

Coloration (Fig. 10A–D): Live specimens brownish red or crimson red. Head and anterior part of metaterga dark brown to brown. Antenna brownish red. Collum, metaterga and epiproct brownish red to crimson red. Paraterga, sternа, surface below paraterga whitish pink; except the middle part of surface below paraterga dark brown. Legs and a few basal podomeres light brown. Coloration in alcohol after two years reddish brown to brown.

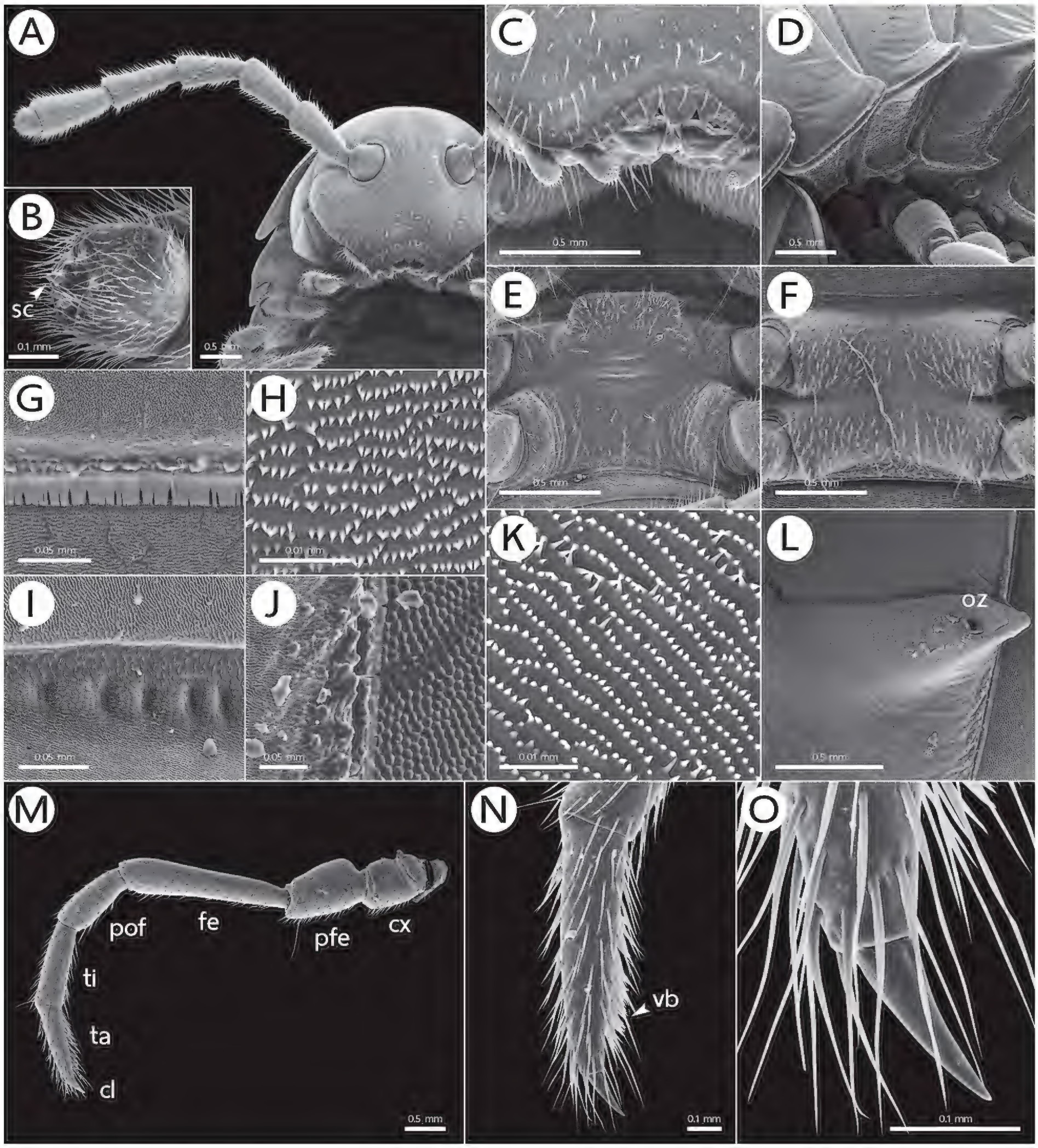

Figure 12. Scanning electron micrographs of *Enghoffosoma rubellum* sp. nov., male paratype (MZKKU-MYR0012). **A.** Head and antenna; **B.** Antennomere 7 and 8; **C.** Clypeus, labrum and tip of gnathochilarium; **D.** Pleurosternal keels on rings 2–4; **E.** Sternal lobe between male coxae 4; **F.** Sternum of ring 10; **G, J.** Surface and limbus between rings 10 and 11, dorsal and lateral views; **H.** Surface of prozona of ring 10; **I.** Stricture between prozona and metazona of ring 10; **K.** Surface below paraterga of ring 10; **L.** Ozopore on paraterga of ring 10; **M.** Male right leg of ring 10; **N.** Ventral brushes on male tarsus; **O.** Claw. Abbreviations: cx = coxa; cl = claw; fe = femur; oz = ozopore; pfe = prefemur; pof = postfemur; sc = sensory cones; ta = tarsus; ti = tibia; vb = ventral brushes.

Head and clypeolabral region (Figs 11K, 12A, C): Vertex entirely bare; epicranial suture conspicuous. Frons sparsely setose. Clypeus and labrum normal.

Antennae (Fig. 12A, B): Short; densely setose; reaching backward to ring 3 (♂) or 2 (♀). In length, antennomeres 2=3>4=6>1>7. Antennomeres 5–7 slightly clavate; each with a group of small sensilla basiconica distally. With four apical cones.

Collum (Fig. 11A, D): Broad and wide. With two transverse rows of inconspicuous setae: 3+3 in anterior position and 1+1 ca. at midlength of collum. Paraterga of collum poorly developed (= obtuse tip).

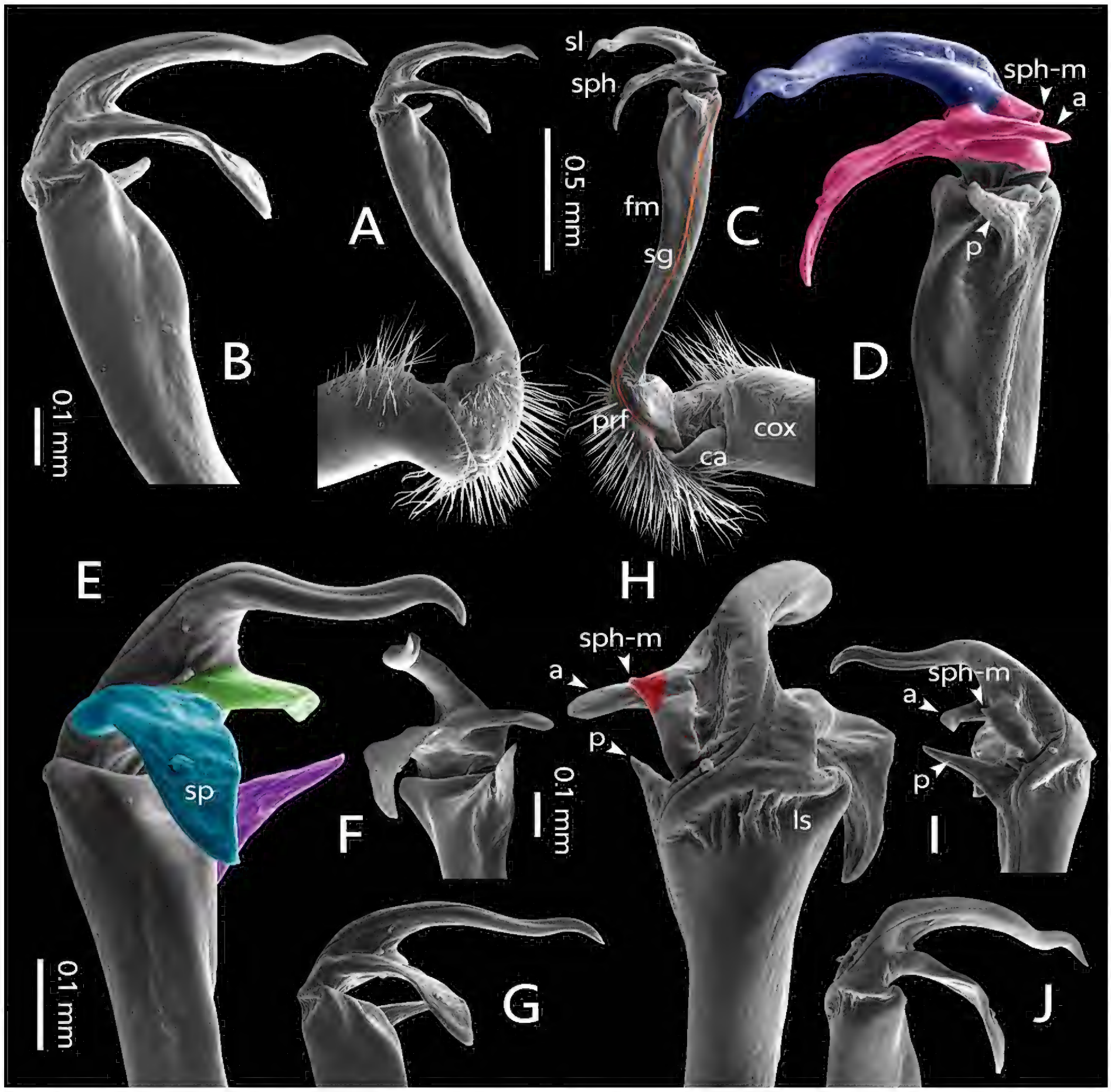

Figure 13. Scanning electron micrographs of *Enghoffosoma rubellum* sp. nov., right gonopod, male paratype (MZKKU-MYR0012). **A, B.** Lateral view; **C, D.** Mesal view; **E.** Ventral view; **F, G.** Subventral view; **H.** Dorsal view; **I, J.** Subdorsal view. Colors: green = process a (a); purple = process on femur (p); orange = seminal groove (sg); navy blue = solenomere (sl); pink = solenophore (sph); sky blue = spatula-like process (sp); red = mesal process on solenophore (sph-m). Abbreviations: a = process; cox = coxa; ca = cannula; fm = femur; ls = lateral sulcus; p = process on femur; pfm = postfemur; prf = prefemur; sg = seminal groove; sl = solenomere; sph = solenophore; sph-m = mesal process on solenophore.

Tegument (Figs 11–F, H, 12K, L): With microspinulation, velvetlike. Prozona, metazona, paraterga and surface below paraterga microspinulate. Prozona on lateral side of body finely shagreened. Stricture between prozona and metazona striolate, quite deep and narrow.

Metaterga (Figs 11H, I, 12I): Metatergum 2–4 with one transverse row of setae (mostly inconspicuous and broken off), 3+3 in anterior position. Metaterga 5–8 with one transverse row of setae, 2+2 in anterior position. Metaterga 9–19 with one transverse row of setae, 1+1 in anterior position. Stricture between prozona and metazona striolate, shallow and narrow. Axial line and transverse sulcus missing.

Limbus (Fig. 12G): Limbus of midbody ring conspicuous; with rows of very long filaments, hairlike, arranged anteroposteriorly; margin finely spiculate; surface in front of limbus with a low and irregular ridge.

Paraterga (Figs 11H, I, 12L): Quite short, stout and small. Paraterga 2–4 short and thin. Paraterga 5–16 stouter and larger than the others. The following paraterga slightly reduced in size and gradually tapering toward telson. No indentation on lateral margin. Posterior corner obtuse, directed caudad. Ozopores small but conspicuous,

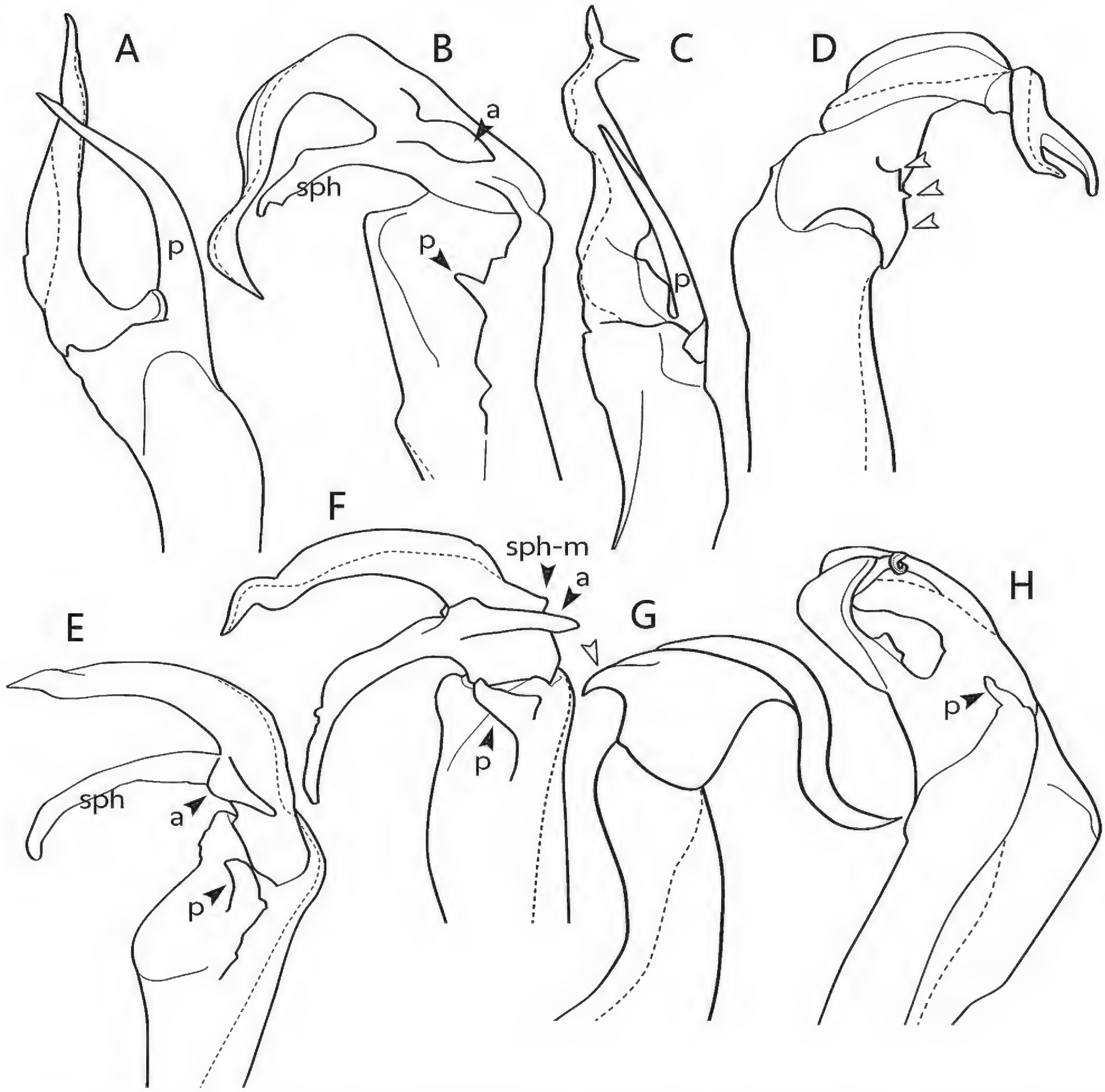

Figure 14. Outline of gonopod telopodite of some *Enghoffosoma* species that show similar conformation in the distal part, all in mesal view. **A.** *E. bispinum* Likhitrakarn et al., 2014; **B.** *E. extraspinosum* Nguyen & Golovatch, 2016; **C.** *E. funda* Likhitrakarn et al., 2014; **D.** *E. furca* sp. nov.; **E.** *E. parvispina* sp. nov.; **F.** *E. rubellum* sp. nov.; **G.** *E. triangulare* Nguyen & Golovatch, 2016; **H.** *E. zebra* Likhitrakarn et al., 2014. Abbreviations: a = process a; p = process p on femur; sph-m = mesal process on solenophore.

oval; present on rings 5, 7, 9, 10, 12, 13, 15–19; visible in lateral view; located near tip of paraterga.

Pleurosternal keels (Figs 11D–F, 12D): Rather well-developed, conspicuous; slightly curved. Keels on rings 2–4 small; rings 2–8 crestlike, with a sharp caudal tooth posteriorly; increasingly reduced to small caudal tooth in rings 9–17; absent in rings 18 and 19.

Telson (Fig. 11J, L, M, N): Preanal ring (epiproct) quite slender, coniform in dorsal view; lateral setiferous tubercles inconspicuous; apical tubercles a little swollen; tip concave; with four spinnerets arranged at the corner without depression. Paraprocts simple, convex. Hypoproct subtriangular; with inconspicuous setiferous tubercles.

Sterna (Fig. 12E, F): Sparsely setose; cross-impressions shallow; posteriorly with a small tubercle near each coxa. Sternal lobe between male coxae 4, broad and large, trapeziform; tip round; with two inconspicuous pores.

Legs (Fig. 12M–O): Moderately long, slender, densely setose; length of midbody leg ca. 4.0–5.1 mm in both sexes; about 1.3 times (♂) or 1.1–1.2 times (♀) as long as midbody height. Prefemur slightly swollen basally. In length, femur > tarsus = tibia = prefemur > postfemur > coxa (♂). Tarsus of legs 1–10 in male with ventral brushes. Claw quite long, slender, pointed. Adenostyles in male absent.

Gonopods (Fig. 13): Coxa (cox) short and stout; with a distoanterior group of setae. Cannula (ca) long and slen-

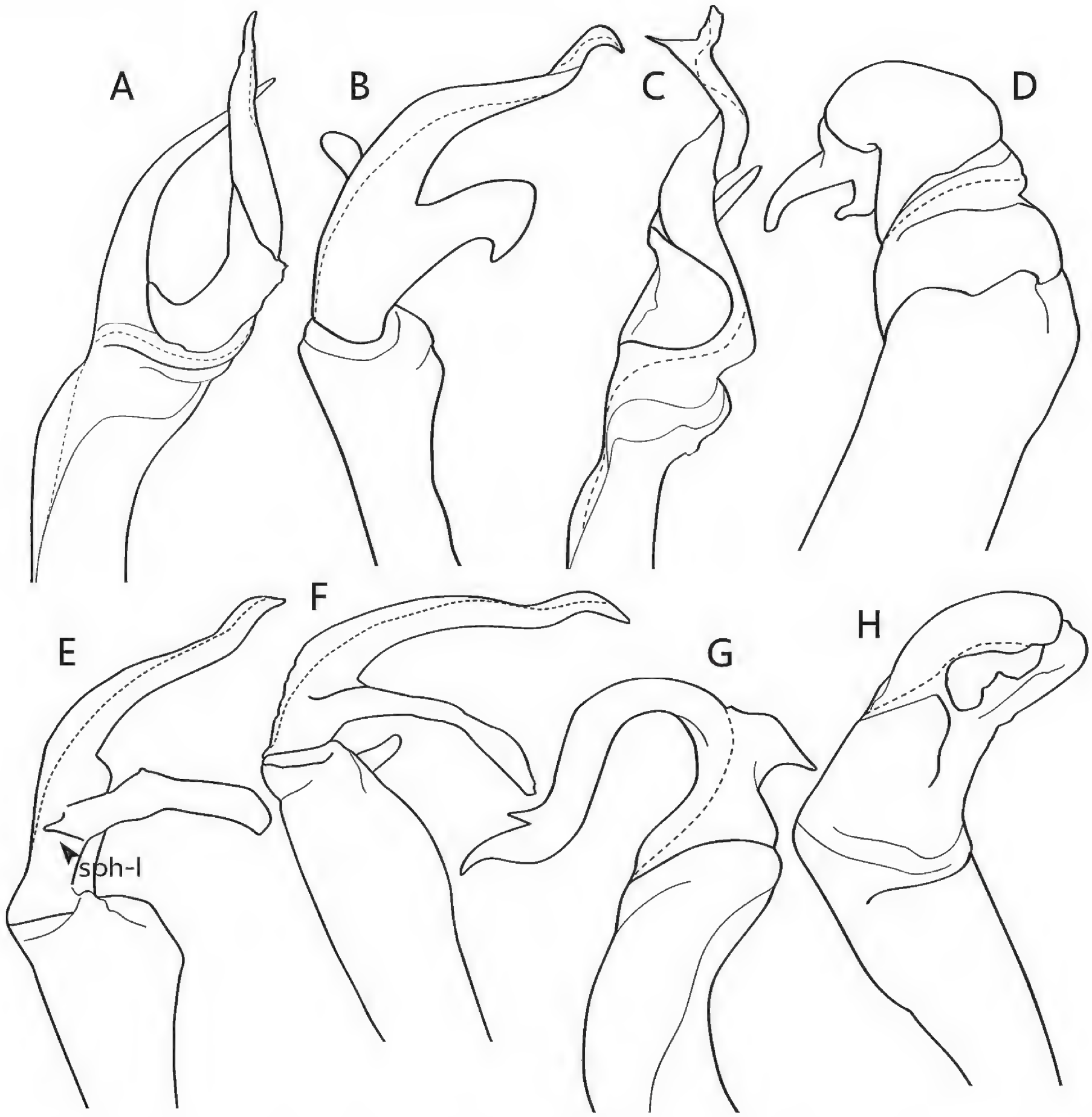

Figure 15. Outline of gonopod telopodite of some *Enghoffosoma* species that show similar conformation in the distal part, all in lateral view **A.** *E. bispinum* Likhitrakarn et al., 2014; **B.** *E. extraspinosum* Nguyen & Golovatch, 2016; **C.** *E. funda* Likhitrakarn et al., 2014; **D.** *E. furca* sp. nov.; **E.** *E. parvispina* sp. nov.; **F.** *E. rubellum* sp. nov.; **G.** *E. triangulare* Nguyen & Golovatch, 2016; **H.** *E. zebra* Likhitrakarn et al., 2014. Abbreviation: sph-l = lateral process on solenophore.

der. Telopodite long and slender; forming a 90° angle with coxa. Prefemur (prf) with dense and long seta; shorter than femur; about 1/3 as long as femur. Femur (fm) very long and slenderer; distally with a long and sharp process (p), digitiform, directed mesad. Seminal groove (sg) running entirely on mesal surface of femur. Lateral sulcus (ls) conspicuous, deep and wide; with 4–5 transverse ridges inside sulcus (Fig. 13H). Mesal sulcus inconspicuous. Postfemoral part (pfm) inconspicuous. Solenophore (sph) well-developed; consisting of three processes. First process (sp) large and very long, spatula-like; tip obtuse, directed posteriad (Fig. 13D, E). Second process (a) smaller and shorter than the first one; slender; located basomesally; tip *in situ* directed dorsolaterad (Fig. 13D, E, H, I). Third process (sph-m) smallest; spinelike; located at base of the second one, clearly seen in dorsal view; tip *in situ* directed mesad (Fig. 13D, H, I). Solenomere (sl) very long and slender; slightly twisted near tip.

Distribution and habitat (Fig. 10E, F). The new species is distributed along the Phu Phan mountain range in Sakon Nakhon Province. All specimens were seen walking and curling their bodies on moist leaf litter in sandstone forest habitat.

Remarks. Among all recorded *Enghoffosoma* species, *E. rubellum* sp. nov. shows such vivid brownish red/red body color that it is easily distinguished from all congeners.

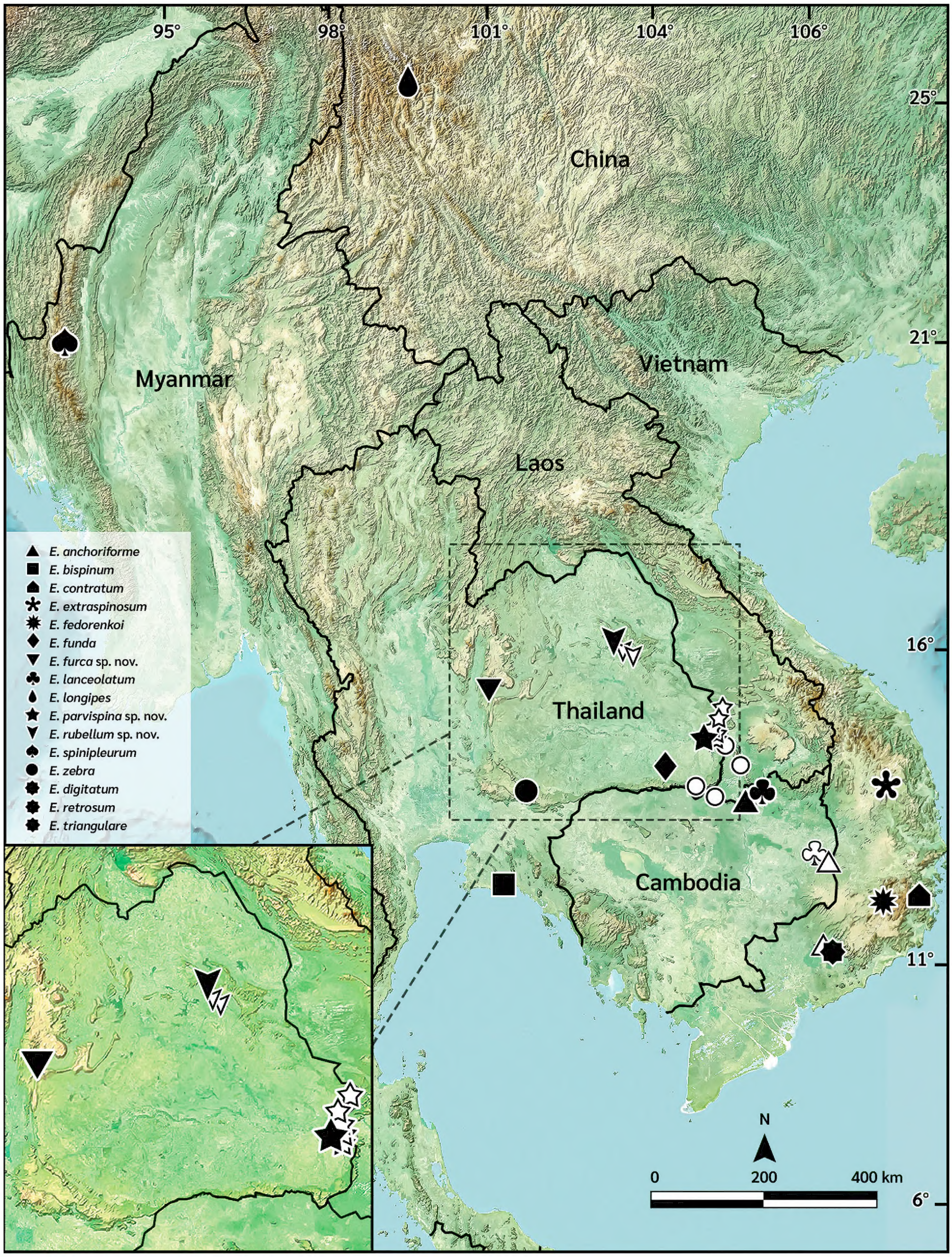

Figure 16. Distribution of all *Enghoffosoma* species. Color of symbol: black = type locality, white = other localities. Inset photo indicates locations of three new species. Type localities of *E. digitatum* Nguyen & Golovatch, 2016, *E. retrosum* Nguyen & Golovatch, 2016 and *E. triangulare* Nguyen & Golovatch, 2016 are in the same location and indicated by the same symbol.

Enghoffosoma zebra Likhitrakarn, Golovatch & Panha, 2014

Enghoffosoma zebra Likhitrakarn, Golovatch & Panha, 2014 in Likhitrakarn et al. 2014: 493.

Enghoffosoma zebra—Nguyen & Golovatch, 2016: 151; Likhitrakarn et al. 2023: 74.

Distribution. Thailand (Nakhon Ratchasima and Ubon Ratchathani provinces) and Laos (Champasak Province).

Remarks. Likhitrakarn et al. (2014) observed variation in the femur of gonopod; some specimens bear a short process (referred to as process p) (Fig. 14H), while others have a longer one.

Discussion

This is the first treatment of the genus *Enghoffosoma* that integrates morphological characteristics and molecular data. It is important to note that the details of the gonopod telopodite clearly differentiate all species from each other. *E. furca* sp. nov. differs from the other species by the presence of three short processes, while *E. parvispina* sp. nov. and *E. rubellum* sp. nov. can be distinguished by the presence of small spinelike processes sph-l and sph-m, at the base of the solenophore, respectively. This aligns with the results of previous studies on paradoxosomatids and xystodesmids, where the integration of morphological and molecular approaches provided sufficient data for accurate species identification (Means et al. 2021; Srisonchai et al. 2024). Other morphological traits such as the color pattern, the sternal lobe on the male coxae 4 and the male tarsal brush can also be used for reliable discrimination. The use of SEM in this study provided deep detail of some informative characters, especially the apical part of the gonopod telopodite. *E. parvispina* sp. nov. and *E. rubellum* sp. nov. both have small spinule-like processes (sph-l and sph-m, respectively) at the base of the solenophore, though these processes arise from different positions: lateral and mesal, respectively. Additionally, *E. extraspinosum* also exhibits a similar process, located midway on a small lobe of the solenophore (Golovatch and Semenyuk 2018).

The interspecific genetic distances of the barcoding COI gene seem to agree with the morphological evidence: the three new species differ significantly from the others, showing high genetic distances of over 15.09% (18.56–22.78% for *E. furca* sp. nov., 15.09–21.25% for *E. parvispina* sp. nov. and 15.09–22.37% for *E. rubellum* sp. nov.). These values closely match the interspecific distances observed in other Paradoxosomatidae, which typically range from 11.4% to above 25% (Decker 2016; Nguyen et al. 2017; Srisonchai et al. 2024). Our phylogenetic tree places *E. parvispina* and *E. rubellum* as separate clades, and *E. furca*, represented by a single terminal, as part of a different lineage, further reinforces the usefulness of gonopod characteristics in distinguishing these species. A discussion of the phylogeny of *Enghoffosoma*, however, is beyond the scope of our current work. To elucidate phylogenetic relationships within *Enghoffosoma* and with their closely related genera, further investigations incorporating additional genetic markers and more taxa is necessary.

The number of described *Enghoffosoma* species found exclusively in Thailand has now reached six. Of these, five species inhabit sandstone environments, while only one is known to occur in limestone habitats. Field surveys conducted between 2020 and 2024 have revealed a greater diversity of *Enghoffosoma* in Thailand than previously thought. These findings indicate that northeastern Thailand is an important area for millipede biodiversity (Fig. 16). It is expected that further exploration in other areas of Thailand, as well as in other countries in the region, like Laos, Cambodia, Myanmar and China, will reveal even more diversity within this genus.

Acknowledgements

The funding for this work was obtained from the National Science, Research and Innovation Fund through the Fundamental Fund of Khon Kaen University (2568), and partly supported by the Office of the Permanent Secretary, Ministry of Higher Education, Science, Research and Innovation (OPS MHESI), Thailand Science Research and Innovation (TSRI) (Grant No. RGNS65-056). The research capability enhancement program through graduate student scholarship (TB), Faculty of Science, Khon Kaen University, is gratefully acknowledged. Thanks are due to staff members of the Department of National Parks, Wildlife and Plant Conservation in Thailand who supported all available surveys in protected areas. We give special gratitude to ASRU and MZKKU colleagues for their assistance in the fieldwork. Special thanks also go to D.J. Anderson for grammar checking and comments. The editor (Luiz Iniesta) and referees (Sergei Golovatch and Dragan Antić) are acknowledged for valuable comments that enormously improved the manuscript. The copy editor (Gabriel Hershman and Bilyana Nikolova) kindly corrected a final version of the manuscript and the CIPRES Science Gateway V 3.3 provided access to computational analysis.

References

American Veterinary Medical Association (2020) AVMA Guidelines for the Euthanasia of Animals: 2020 edn. https://www.avma.org/sites/default/files/2020-02/Guidelines-on-Euthanasia-2020.pdf

Darriba D, Taboada GL, Doallo R, Posada D (2012) jModelTest 2: more models, new heuristics and parallel computing. Nature Methods 9: 772. https://doi.org/10.1038/nmeth.2109

Decker P (2016) Integrative taxonomic revision of the polymorphic flat-millipede genera *Oncocladosoma* and *Somethus* in South Australia (Diplopoda: Polydesmida: Paradoxosomatidae). Invertebrate Systematics 30(3): 201–218. https://doi.org/10.1071/IS15047

Folmer O, Black M, Hoeh W, Lutz R, Vrijenhoek R (1994) DNA primers for amplification of mitochondrial cytochrome c oxidase subunit

I from diverse metazoan invertebrates. Molecular Marine Biology and Biotechnology 3: 294–299.

Golovatch SI (1993) On several new or poorly-known Oriental Paradoxosomatidae (Diplopoda Polydesmida). Arthropoda Selecta 2(1): 3–14. https://doi.org/10.15298/arthsel.30.1.01

Golovatch SI (2011) On several new or poorly-known Oriental Paradoxosomatidae (Diplopoda: Polydesmida), XI. Arthropoda Selecta 20(1): 259–266. https://doi.org/10.15298/arthsel.20.4.02

Golovatch SI (2016) On several new or poorly-known Oriental Paradoxosomatidae (Diplopoda: Polydesmida), XIX. Arthropoda Select 25(2): 131–152. https://doi.org/10.15298/arthsel.25.2.01

Golovatch SI, Semenyuk I (2018) On several new or poorly-known oriental paradoxosomatidae (Diplopoda: Polydesmida), XXIII. Arthropoda Selecta 27(1): 1–21. https://doi.org/10.15298/arthsel.27.1.01

Golovatch SI, VandenSpiegel D, Semenyuk II (2016) On several new or poorly-known Oriental Paradoxosomatidae (Diplopoda: Polydesmida), XXI. Arthropoda Selecta 25(4): 335–354. https://doi.org/10.15298/arthsel.25.4.01

Hillis DM, Bull JJ (1993) An empirical test of bootstrapping as a method for assessing confidence in phylogenetic analysis. Systematic Biology 42(2): 182–192. https://doi.org/10.1093/sysbio/42.2.182

Huelsenbeck JP, Rannala B (2004) Frequentist properties of Bayesian posterior probabilities of phylogenetic trees under simple and complex substitution models. Systematic Biology 53(6): 904–913. https://doi.org/10.1080/10635150490522629

Likhitrakarn N, Golovatch SI, Prateepasen R, Panha S (2010) Review of the genus *Tylopus* Jeekel, 1968, with descriptions of five new species from Thailand (Diplopoda, Polydesmida, Paradoxosomatidae). ZooKeys 72: 23–68. https://doi.org/10.3897/zookeys.72.744

Likhitrakarn N, Golovatch SI, Panha S (2011) Revision of the Southeast Asian millipede genus *Orthomorpha* Bollman, 1893, with the proposal of a new genus (Diplopoda, Polydesmida, Paradoxosomatidae). ZooKeys 131: 1–161. https://doi.org/10.3897/zookeys.131.1921

Likhitrakarn K, Golovatch SI, Panha S (2014) Review of the Southeast Asian millipede genus *Enghoffosoma* Golovatch, 1993 (Diplopoda, Polydesmida, Paradoxosomatidae), with descriptions of new species. Zootaxa 3811(4): 491–514. https://doi.org/10.11646/zootaxa.3811.4.4

Likhitrakarn N, Golovatch SI, Semenyuk I, Efeykin BD, Panha S (2019) Review of the millipede genus *Orthomorpha* Bollman, 1893 (Diplopoda, Polydesmida, Paradoxosomatidae) in Vietnam, with several new records and descriptions of two new species. ZooKeys 898: 121–158. https://doi.org/10.3897/zookeys.898.39265

Likhitrakarn N, Srisonchai R, Golovatch SI (2023) An updated catalogue of the millipedes (Diplopoda) of Thailand. Tropical Natural History 7: 51–92. https://li01.tcithaijo.org/index.php/tnh/article/view/258815

Means JC, Hennen DA, Marek PE (2021) A revision of the minor species group in the millipede genus *Nannaria* Chamberlin, 1918 (Diplopoda, Polydesmida, Xystodesmidae). ZooKeys 1030(1): 1–180. https://doi.org/10.3897/zookeys.1030.62544

Miller MA, Pfeiffer W, Schwartz T (2010) Creating the CIPRES Science Gateway for inference of large phylogenetic trees. In 'Proceedings of the Gateway Computing Environments Workshop (GCE)', 14 November 2010, New Orleans, LA, USA. INSPEC 11705685, 1–8. https://doi.org/10.1109/GCE.2010.5676129

Minh BQ, Schmidt HA, Chernomor O, Schrempf D, Woodhams MD, von Haeseler A, Lanfear R (2020) IQ-TREE 2: New models and efficient methods for phylogenetic inference in the genomic era. Molecular Biology and Evolution 37: 1530–1534. https://doi.org/10.1093/molbev/msaa015

Nguyen AD, Golovatch SI (2016) The millipede genus *Enghoffosoma* Golovatch, 1993 recorded in Vietnam for the first time, with descriptions of three new species (Diplopoda, Polydesmida, Paradoxosomatidae). Zootaxa 4139(2): 151–166. https://doi.org/10.11646/zootaxa.4139.2.1

Nguyen AD, Sierwald, P. (2013) A worldwide catalog of the family Paradoxosomatidae Daday, 1889 (Diplopoda: Polydesmida). CheckList 9(6): 1132–1353. https://doi.org/10.15560/9.6.1132

Nguyen AD, Korsós Z, Jang KH, Hwang UW (2017) A revision and phylogenetic analysis of the millipede genus *Oxidus* Cook, 1911 (Polydesmida, Paradoxosomatidae). European Journal of Taxonomy 293: 1–22. https://doi.org/10.5852/ejt.2017.293

Nguyen AD, Nguyen SG, Le SX (2018) On the millipede genus *Antheromorpha* Jeekel, 1968 (Diplopoda: Polydesmida: Paradoxosomatidae) from Vietnam, with a description of a new species. Raffles Bulletin of Zoology 66: 96–109.

Pimvichai P, Enghoff H, Panha S (2009) A revision of the *Thyropygus allevatus* group. Part 1: the *T. opinatus* subgroup (Diplopoda: Spirostreptida: Harpagophoridae). Zootaxa 2016(1): 17–50. https://doi.org/10.11646/zootaxa.2016.1.2

Pimvichai P, Enghoff H, Panha S (2014) Molecular phylogeny of the *Thyropygus allevatus* group of giant millipedes and some closely related groups. Molecular Phylogenetics and Evolution 71: 170–183. https://doi.org/10.1016/j.ympev.2013.11.006

Rambaut A (2018) Figtree ver 1.4.4. Institute of Evolutionary Biology, University of Edinburgh, Edinburgh. http://tree.bio.rd.ac.uk/software/figtree [Accessed at 27 December 2023]

Ronquist F, Teslenko M, van der Mark P, Ayres DL, Darling A, Höhna S, Larget B, Liu L, Suchard MA, Huelsenbeck JP (2012) MrBayes 3.2: Efficient Bayesian phylogenetic inference and model choice across a large model space. Systematic Biology 61: 539–542. https://doi.org/10.1093/sysbio/sys029

Srisonchai R, Enghoff H, Likhitrakarn N, Panha S (2018) A revision of dragon millipedes I: genus *Desmoxytes* Chamberlin, 1923, with the description of eight new species (Diplopoda, Polydesmida, Paradoxosomatidae). ZooKeys 761: 1–177. https://doi.org/10.3897/zookeys.761.24214

Srisonchai R, Inkhavilay K, Ngor PB, Sutcharit C, Likhitrakarn N (2023) Uncovering endemism in high montane forests: Two new species of millipede genus *Tylopus* Jeekel, 1968 (Diplopoda: Polydesmida: Paradoxosomatidae) from Cambodia and Laos.Tropical Natural History 1(7): 151–164.

Srisonchai R, Enghoff H, Likhitrakarn N, Jeratthitikul E, Jirapatrasilp P, Panha S, Sutcharit C (2024) Molecular phylogeny of dragon millipedes (Diplopoda: Polydesmida: Paradoxosomatidae) from mainland South-East Asia, with description of a new genus and species. Zoological Journal of the Linnean Society 202(1): zlad164. https://doi.org/10.1093/zoolinnean/zlad164

Tamura K, Stecher G, Kumar S (2021) MEGA11: molecular evolutionary genetics analysis version 11. Molecular Biology and Evolution 38(7): 3022–3027. https://doi.org/10.1093/molbev/msab120

Tanabe AS (2011) Kakusan4 and Aminosan: two programs for comparing nonpartitioned, proportional and separate models for combined molecular phylogenetic analyses of multilocus sequence data. Molecular Ecology Resources 11: 914–921. https://doi.org/10.1111/j.1755-0998.2011.03021.x

Supplementary material 1

List of species names used in this study and their COI accession numbers

Authors: Theemaporn Benchapong, Henrik Enghoff, Natdanai Likhitrakarn, Ratmanee Chanabun, Anuwat Aoonkum, Ruttapon Srisonchai

Data type: docx

Copyright notice: This dataset is made available under the Open Database License (http://opendatacommons.org/licenses/odbl/1.0/). The Open Database License (ODbL) is a license agreement intended to allow users to freely share, modify, and use this Dataset while maintaining this same freedom for others, provided that the original source and author(s) are credited.

Link: https://doi.org/10.3897/zse.101.144277.suppl1

Supplementary material 2

Uncorrected *p*-distances of cytochrome c oxidase subunit I (COI) sequence divergences in the genus *Enghoffosoma*

Authors: Theemaporn Benchapong, Henrik Enghoff, Natdanai Likhitrakarn, Ratmanee Chanabun, Anuwat Aoonkum, Ruttapon Srisonchai

Data type: xlsx

Copyright notice: This dataset is made available under the Open Database License (http://opendatacommons.org/licenses/odbl/1.0/). The Open Database License (ODbL) is a license agreement intended to allow users to freely share, modify, and use this Dataset while maintaining this same freedom for others, provided that the original source and author(s) are credited.

Link: https://doi.org/10.3897/zse.101.144277.suppl2